

# Realistic fast quantum gates with hot trapped ions

Marek Šašura<sup>1,2</sup> and Andrew M. Steane<sup>1</sup>

<sup>1</sup>*Centre for Quantum Computation, Clarendon Laboratory,  
Department of Physics, University of Oxford, Parks Road, Oxford OX1 3PU, UK*

<sup>2</sup>*Research Center for Quantum Information (RCQI), Institute of Physics,  
Slovak Academy of Sciences, Dúbravská cesta 9, Bratislava 842 28, Slovakia*

(Dated: December 2, 2002)

The “pushing gate” proposed by Cirac and Zoller for quantum logic in ion traps is discussed, in which a force is used to give a controlled push to a pair of trapped ions and thus realize a phase gate. The original proposal had a weakness in that it involved a hidden extreme sensitivity to the size of the force. Also, the physical origin of this force was not fully addressed. Here, we discuss the sensitivity and present a way to avoid it by choosing the spatial form of the pushing force in an optimal way. We also analyse the effect of imperfections in a pair of  $\pi$  pulses which are used to implement a “spin-echo” to cancel correlated errors. We present a physical model for the force, namely the dipole force, and discuss the impact of unwanted photon scattering, and of finite temperature of the ions. The main effect of the temperature is to blur the phase of the gate owing to the ions exploring a range of values of the force. When the distance scale of the force profile is smaller than the ion separation this effect is more important than the high-order terms in the Coulomb repulsion which were originally discussed. Overall, we find that whereas the “pushing gate” is not as resistant to imperfection as was supposed, it remains a significant candidate for ion trap quantum computing since it does not require ground state cooling, and in some cases it does not require the Lamb-Dicke limit, while the gate rate is fast, close to (rather than small compared to) the trap vibrational frequency.

PACS numbers: 03.67.-a, 42.50.-p

## I. INTRODUCTION

Since the first recognition of the advantages of ion traps for quantum computing [1], various proposals to achieve quantum gates between pairs of trapped ions have been put forward [2]. In all cases each ion stores one or more qubits in its internal state, and most proposals have envisaged two or more ions in the same harmonic well, with the joint motional degree of freedom (normal mode of oscillation) serving as a further carrier of quantum information, which can be coupled to any chosen ion by laser excitation [3–6]. More recently a method of a qualitatively different form was proposed, in which the ions need not be in the same harmonic well, and a quantum gate is achieved through a more direct use of the Coulomb repulsion between ions [7]. Two ions in neighbouring harmonic wells are pushed by a force which depends on their internal state. Therefore, their mean separation depends on their internal state while the force acts. It is shown in Ref. [8] that the phase acquired from the Coulomb energy has the form of single-qubit rotations combined with the controlled-phase gate  $|00\rangle\langle 00| + |01\rangle\langle 01| + |10\rangle\langle 10| + e^{i\theta} |11\rangle\langle 11|$ . This “pushing gate” is significant for three reasons. First, it was shown [8] that in the right conditions the gate is unusually insensitive to the details of the motion of the ions, i.e. the quantum phases depend primarily on the mean positions of the ions, and are insensitive, for example, to the ion temperature. Secondly, the gate can be faster than those previously proposed. Thirdly, the fact that the gate can act on ions in separate wells is useful for

scaling the computer up to large numbers of ions, because it is possible to move the ions around without ever having to “tease apart” two ions which were initially in the same well.

For these reasons the “pushing gate” is a promising idea, but various aspects were left unclear in work up till now, as follows.

(i) The method generates single-qubit rotations simultaneously with the desired two-qubit phase gate. In the original work [8] it was assumed that these rotations would be unproblematic, since they are known from the experimental parameters and can be undone afterwards, if so desired, by any available single-qubit gate method. Therefore, the explicit calculation of these phases was not carried out. However, if the rotation angles are large compared to  $\pi$  they will be sensitive to experimental imprecision. Therefore, it is necessary to calculate them and if possible, find ways to suppress or compensate for them.

(ii) A state-dependent pushing force was introduced without analysing in sufficient detail the physical mechanism which gives rise to the force.

(iii) The proposal assumed that the force is independent of position, and it was unclear to what extent the good behaviour of the gate relied on that assumption.

(iv) The effect of imprecision or fluctuations in the parameters was not considered.

The reason it is important to clarify these points is that until this is done, it is not clear whether the good performance of the gate is genuine, or whether it is an artifact of some unphysical assumption, such as an unrea-

sonably high laser intensity or an unreasonably high precision in parameters. This paper will address the points just listed.

In Sec. II we introduce the basic concept of a generalised phase gate in order to bring out the physics without reference to any specific physical system. We also examine the double  $\pi$ -pulse “spin-echo” which was suggested in Ref. [8] as a way to improve the fidelity. The “spin-echo” is used to cancel a correlated error which might be large, so there is a danger that a small imprecision in this part of the evolution might result in a large loss of fidelity. Therefore, we examine the influence of imprecision in the  $\pi$  pulses.

In Sec. III we introduce the ion trap system. First, we show how the gate works in a qualitative way, and then we write down the Hamiltonian and deduce the classical trajectories of the ions under the influence of the two trapping potentials, their Coulomb repulsion, and the state-selective and time-dependent pushing force which is, for this section, assumed to be independent of position.

Sec. IV then obtains all the quantum phases which arise in the evolution in the semiclassical approximation, where the trajectories are classical and the quantum phase is obtained from a path integral along the classical trajectory. Our main purpose is to obtain the single-qubit rotation phases which were not calculated in the original paper [8]. In order to make the treatment self-contained we also rederive the two-qubit phase which is the central feature of the gate.

Sec. V considers an explicit choice for the pushing force. The most natural choice is the dipole force from a non-resonant laser beam. This has the unavoidable consequence that unwanted scattering of photons will occur, which reduces the fidelity. We calculate the photon scattering and hence the loss of fidelity.

In Sec. VI we examine the influence of fluctuations in the laser intensity. This is important because the single-qubit phases introduced by the gate are large, so that in some parameter regimes small changes in laser intensity can cause single-qubit rotations much larger than  $\pi$ , destroying the fidelity. We propose a way to largely circumvent this problem by appropriately choosing the directions of the forces and the distance scale of the potential energy function (e.g. AC Stark light shifts), which provides the force.

In Sec. VII we examine the effect of position dependence of the force, which is a major constraint on the temperature of the ions. It is also non-negligible since tightly focused laser beams, or a laser standing wave, must be used to get sufficient dipole force without unreasonably high laser power.

In Sec. VIII we consider the total fidelity of the gate, including the effects of imperfect  $\pi$  pulses, photon scattering, positional dependence of the force, and non-zero temperature of the ions. We give example values for the calcium ion, and discuss the results in comparison to other gate methods in ion traps.

## II. GENERAL CONCEPT

In this section we shall introduce a general concept of a two-qubit phase gate. We discuss the fidelity of the phase gate and also the fidelity of the gate incorporating a double  $\pi$ -pulse or “spin-echo” method to cancel one source of infidelity. Finally, we treat the latter case with imperfect  $\pi$  pulses.

### A. Phase gate

Consider a system of two interacting qubits described by the evolution operator  $G$  in the computational basis  $\{|00\rangle, |01\rangle, |10\rangle, |11\rangle\}$  having the form

$$G = \sum_{\alpha, \beta=0}^1 |\alpha\beta\rangle\langle\alpha\beta| e^{i\Theta_{\alpha\beta}} \\ = \text{diag}\{e^{i\Theta_{00}}, e^{i\Theta_{01}}, e^{i\Theta_{10}}, e^{i\Theta_{11}}\}, \quad (1)$$

where the phases  $\Theta_{\alpha\beta}$  have different values in general because the states  $|\alpha\beta\rangle \equiv |\alpha\rangle_1 \otimes |\beta\rangle_2$  can have a different energy during the interaction and hence a different action integral. A physical system which satisfies the evolution (1) will be introduced and described in Sec. III.

The operation  $G$  can be transformed into a two-qubit phase gate  $P_{\vartheta}$  which generates a phase  $\vartheta$  if and only if both qubits are in the logical state  $|1\rangle$ , that is

$$P_{\vartheta} = \text{diag}\{1, 1, 1, e^{i\vartheta}\}. \quad (2)$$

The transformation  $G \rightarrow P_{\vartheta}$  can be accomplished by local operations (single-qubit rotations) applied on each qubit

$$S = S_1 \otimes S_2, \quad (3)$$

with

$$S_1 = Z_1(\Theta_{10} - \Theta_{00}), \quad (4a)$$

$$S_2 = Z_2(\Theta_{01} - \Theta_{00}), \quad (4b)$$

where

$$Z_j(\Theta) \equiv |0\rangle_j\langle 0| e^{i\Theta/2} + |1\rangle_j\langle 1| e^{-i\Theta/2} \quad (5)$$

is a rotation by the angle  $\Theta$  about the  $z$  axis of the Bloch sphere. Bringing together Eq. (1) and (3) we can realise the phase gate (2) in the following way

$$\begin{aligned} |00\rangle &\xrightarrow{G} e^{i\Theta_{00}} |00\rangle \xrightarrow{S} |00\rangle, \\ |01\rangle &\longrightarrow e^{i\Theta_{01}} |01\rangle \longrightarrow |01\rangle, \\ |10\rangle &\longrightarrow e^{i\Theta_{10}} |10\rangle \longrightarrow |10\rangle, \\ |11\rangle &\longrightarrow e^{i\Theta_{11}} |11\rangle \longrightarrow e^{i\vartheta} |11\rangle, \end{aligned} \quad (6)$$

where

$$\vartheta = \Theta_{11} - \Theta_{10} - \Theta_{01} + \Theta_{00}, \quad (7)$$

and a global phase  $(\Theta_{01} + \Theta_{10})/2$  was neglected. The two-qubit phase gate with the phase  $\vartheta = \pi$  is equivalent (up to additional single-qubit rotations) to a two-qubit controlled-NOT (CNOT) gate, which together with single-qubit rotations forms a universal set of gates for quantum computation [9].

### B. Imprecision of the phase gate

In practice for a particular physical system the phases  $\Theta_{\alpha\beta}$  in Eq. (1) are not accurately known and they may vary from one realisation of the gate to another. On the other hand, we can assume the single-qubit rotations (4) are applied with a very high accuracy. A good choice for the phases  $\Theta_{\alpha\beta}$  in Eq. (4) is obtained by estimating the most likely values of these phases which will occur during the gate operation (1). We denote this choice in the following way

$$\begin{aligned} \Theta_{00} &\rightarrow \bar{\Theta}_{00}, & \Theta_{01} &\rightarrow \bar{\Theta}_{01}, \\ \Theta_{10} &\rightarrow \bar{\Theta}_{10}, & \Theta_{11} &\rightarrow \bar{\Theta}_{11}. \end{aligned} \quad (8)$$

Then, the actual gate is not a perfect gate but it is rather the transformation

$$\begin{aligned} |00\rangle &\xrightarrow{G} e^{i\Theta_{00}} |00\rangle \xrightarrow{S} e^{i(\Theta_{00} - \bar{\Theta}_{00})} |00\rangle, \\ |01\rangle &\longrightarrow e^{i\Theta_{01}} |01\rangle \longrightarrow e^{i(\Theta_{01} - \bar{\Theta}_{01})} |01\rangle, \\ |10\rangle &\longrightarrow e^{i\Theta_{10}} |10\rangle \longrightarrow e^{i(\Theta_{10} - \bar{\Theta}_{10})} |10\rangle, \\ |11\rangle &\longrightarrow e^{i\Theta_{11}} |11\rangle \longrightarrow e^{i\bar{\vartheta}} e^{i(\Theta_{11} - \bar{\Theta}_{11})} |11\rangle, \end{aligned} \quad (9)$$

where we denoted

$$\bar{\vartheta} = \bar{\Theta}_{11} - \bar{\Theta}_{10} - \bar{\Theta}_{01} + \bar{\Theta}_{00}, \quad (10)$$

and we will require  $\bar{\vartheta} = \pi$ . The precision of the gate is limited by the degree to which  $G$  is not perfectly predictable from one realisation of the gate to another, owing to technical noise and the finite temperature of the trapped ions.

### C. Fidelity of the phase gate

In order to calculate the fidelity of the phase gate we have to compare an output state of a perfect gate and an actual gate. We will define the fidelity as follows

$$\mathcal{F} = \langle \min |\langle \Psi_{\text{perf}} | \Psi_{\text{act}} \rangle|^2 \rangle, \quad (11)$$

where the perfect state is produced by the perfect phase gate (2) for  $\vartheta = \pi$ , giving

$$|\Psi_{\text{perf}}\rangle = P_{\pi} |\Psi_0\rangle, \quad (12)$$

while the actual state follows from the actual gate given by the transformation (9), that is

$$|\Psi_{\text{act}}\rangle = SG |\Psi_0\rangle. \quad (13)$$

We assume a general initial state

$$|\Psi_0\rangle = \sum_{\alpha, \beta=0}^1 c_{\alpha\beta} |\alpha\beta\rangle, \quad (14)$$

the minimisation in Eq. (11) runs over all possible initial states  $|\Psi_0\rangle$  and  $\langle \cdot \rangle$  denotes averaging over other degrees of freedom of the system. The imperfection in  $G$  can be expressed by an *error operator*  $E$  defined through

$$G = EG_{\text{perf}} = E(S^{\dagger} P_{\bar{\vartheta}}), \quad (15)$$

where we used the relation  $P_{\bar{\vartheta}} = SG_{\text{perf}}$ . It follows from Eq. (15) that

$$E = \text{diag} \{ e^{i\delta\Theta_{00}}, e^{i\delta\Theta_{01}}, e^{i\delta\Theta_{10}}, e^{i\delta\Theta_{11}} \}, \quad (16)$$

$$G_{\text{perf}} = \text{diag} \{ e^{i\bar{\Theta}_{00}}, e^{i\bar{\Theta}_{01}}, e^{i\bar{\Theta}_{10}}, e^{i\bar{\Theta}_{11}} \}, \quad (17)$$

written in the basis  $\{|00\rangle, |01\rangle, |10\rangle, |11\rangle\}$  and we introduced the notation

$$\delta\Theta_{\alpha\beta} \equiv \Theta_{\alpha\beta} - \bar{\Theta}_{\alpha\beta}. \quad (18)$$

Bringing together Eq. (12), (13) and (15) we obtain

$$\begin{aligned} |\langle \Psi_{\text{perf}} | \Psi_{\text{act}} \rangle|^2 &= |\langle \Psi_0 | P_{\pi}^{\dagger} S G | \Psi_0 \rangle|^2 \\ &= |\langle \Psi_0 | P_{\pi}^{\dagger} S (E S^{\dagger} P_{\bar{\vartheta}}) | \Psi_0 \rangle|^2 \\ &= |\langle \Psi_0 | E | \Psi_0 \rangle|^2, \end{aligned} \quad (19)$$

where we used the commutation of diagonal operators and we assumed  $\bar{\vartheta} = \pi$  in order to accomplish the desired gate. Hence the fidelity is

$$\mathcal{F} = \left\langle \min_{\{c_{\alpha\beta}\}} \left| \sum_{\alpha, \beta=0}^1 |c_{\alpha\beta}|^2 e^{i\delta\Theta_{\alpha\beta}} \right|^2 \right\rangle. \quad (20)$$

The phases  $\delta\Theta_{\alpha\beta}$  are random variables and to obtain a single fidelity measure it is necessary to average over characteristic probability distributions (associated with other degrees of freedom of the system).

### D. $\pi$ -pulse method

The general concept in Eq. (1)–(7) of factoring a general phase rotation into single-qubit and two-qubit terms can be applied to the error operator  $E$ , giving

$$E = Z_1(\delta\Theta_{00} - \delta\Theta_{10}) Z_2(\delta\Theta_{00} - \delta\Theta_{01}) P_{\delta\vartheta}, \quad (21)$$

where we refer to the notation in Eq. (18), we denoted  $\delta\vartheta = \vartheta - \bar{\vartheta}$  and we dropped a global phase  $(-\delta\Theta_{01} - \delta\Theta_{10})/2$ . We now consider a method which can be used to suppress the single-qubit rotations in the error operator  $E$ , leaving only the part which depends on  $\delta\vartheta$ . This method uses a pair of  $\pi$  pulses on qubits 1 and 2 of the form

$$R = R_1 \otimes R_2, \quad (22)$$

where

$$R_1 = |0\rangle_1\langle 1| - |1\rangle_1\langle 0|, \quad (23a)$$

$$R_2 = |0\rangle_2\langle 1| - |1\rangle_2\langle 0|. \quad (23b)$$

We replace the gate sequence  $SG$  in Eq. (9) by  $S'(RG)^2$ , to obtain

$$\begin{aligned} |00\rangle &\xrightarrow{S'(RG)^2} e^{i(\delta\Theta_{00}+\delta\Theta_{11})} |00\rangle, \\ |01\rangle &\longrightarrow e^{i(\delta\Theta_{01}+\delta\Theta_{10})} |01\rangle, \\ |10\rangle &\longrightarrow e^{i(\delta\Theta_{10}+\delta\Theta_{01})} |10\rangle, \\ |11\rangle &\longrightarrow e^{i2\bar{\vartheta}} e^{i(\delta\Theta_{11}+\delta\Theta_{00})} |11\rangle, \end{aligned} \quad (24)$$

where we used the notation (18),  $R$  is defined in Eq. (22),  $G$  is given by Eq. (1) and

$$S' = S'_1 \otimes S'_2, \quad (25)$$

with

$$S'_i = Z_i(-\bar{\vartheta}) \quad (26)$$

where  $i = 1, 2$  and a global phase  $\bar{\Theta}_{01} + \bar{\Theta}_{10}$  has been dropped in Eq. (24). Comparing Eq. (9) and (24), it can be seen that the joint logical state  $|11\rangle$  is rotated during the new gate sequence by  $2\bar{\vartheta}$ , so now we require  $2\bar{\vartheta} = \pi$ . This means that in the new sequence (24) each operation  $G$  will typically be applied for a time half as long as in the sequence (9).

### E. Fidelity of the phase gate using the $\pi$ -pulse method

When we use the gate sequence with the  $\pi$  pulses in Eq. (24), the actual state of the qubits is

$$|\Psi_{\text{act}}\rangle = S'(RG)^2|\Psi_0\rangle, \quad (27)$$

while the perfect state is given again by Eq. (12). Then, the fidelity of the gate with the perfect  $\pi$  pulses turns out to be

$$\mathcal{F}' = \left\langle \min_{\{c_{\alpha\beta}\}} \left| \sum_{\alpha,\beta=0}^1 |c_{\alpha\beta}|^2 e^{i(\delta\Theta_{\alpha\beta}+\delta\Theta_{\alpha'\beta'})} \right|^2 \right\rangle, \quad (28)$$

where  $\alpha' \equiv 1 - \alpha$  and  $\beta' \equiv 1 - \beta$ . We prove this in the following (note that Eq. (28) and (37) are identical). Whenever  $\delta\Theta_{\alpha\beta} \ll 1$  and  $\delta\Theta_{\alpha\beta} + \delta\Theta_{\alpha'\beta'} \ll \delta\Theta_{\alpha\beta}$ , we achieve a significant improvement in the fidelity of the phase gate using the  $\pi$  pulses, that is  $1 - \mathcal{F}' \ll 1 - \mathcal{F}$ .

The way the  $\pi$ -pulse method works can be brought out by writing the gate sequence (24) using the error operator expressed in Eq. (21). That is

$$\begin{aligned} S'(RG)^2 &= S'(REG_{\text{perf}})^2 \\ &= S'[R_1R_2Z_1(\phi)Z_2(\phi')P_{\delta\vartheta}G_{\text{perf}}]^2, \end{aligned} \quad (29)$$

where the phases  $\phi$  and  $\phi'$  are given in Eq. (21), but now we do not need to know what they are since we are about to prove that they cancel. Expressing the rotations using Pauli matrices, we have

$$Z_j(\phi) = \cos(\phi/2)\mathbb{1}_j + \sin(\phi/2)(\sigma_z)_j, \quad (30)$$

$$R_j = i(\sigma_y)_j \quad (31)$$

for  $j = 1, 2$ . Since  $\sigma_y$  commutes with  $\mathbb{1}$  and anticommutes with  $\sigma_z$ , we can write

$$R_j Z_j(\phi) = Z_j(-\phi) R_j. \quad (32)$$

The operators  $Z_j(\phi)$ ,  $P_{\delta\vartheta}$  and  $G_{\text{perf}}$  all commute, since they are diagonal, so the rotations  $Z_j(\phi)$  cancel out in Eq. (29) because they appear twice in the sequence with opposite sign (after using Eq. (32)). Then we get

$$S'[R_1R_2Z_1(\phi)Z_2(\phi')P_{\delta\vartheta}G_{\text{perf}}]^2 = S'(RP_{\delta\vartheta}G_{\text{perf}})^2. \quad (33)$$

The fidelity of the phase gate using the  $\pi$ -pulse method is

$$\mathcal{F}' = \left\langle \min_{|\Psi_0\rangle} \left| \langle \Psi_0 | [(G_{\text{perf}}^\dagger R^\dagger)^2 (S')^\dagger] [S'(RG)^2] | \Psi_0 \rangle \right|^2 \right\rangle. \quad (34)$$

Using Eq. (29) and (33) this becomes

$$\begin{aligned} \mathcal{F}' &= \left\langle \min_{|\Psi_0\rangle} \left| \langle \Psi_0 | (G_{\text{perf}}^\dagger R^\dagger)^2 (RP_{\delta\vartheta}G_{\text{perf}})^2 | \Psi_0 \rangle \right|^2 \right\rangle \\ &= \left\langle \min_{|\Psi_0\rangle} \left| \langle \Psi_0 | G_{\text{perf}}^\dagger (RP_{\delta\vartheta})^2 G_{\text{perf}} | \Psi_0 \rangle \right|^2 \right\rangle, \end{aligned} \quad (35)$$

where we applied  $R^\dagger = R$ . Let us introduce

$$E' \equiv (RP_{\delta\vartheta})^2 = \text{diag}\{e^{i\delta\vartheta}, 1, 1, e^{i\delta\vartheta}\}. \quad (36)$$

Hence, the error operator  $E'$  is diagonal so it commutes with  $G_{\text{perf}}$ , giving

$$\mathcal{F}' = \left\langle \min |\langle \Psi_0 | E' | \Psi_0 \rangle|^2 \right\rangle. \quad (37)$$

Clearly, when the uncertainties in the phases are such that the combination  $\vartheta$  has an uncertainty  $\delta\vartheta$  small compared to the uncertainties in the individual phases  $\delta\Theta_{\alpha\beta}$  in Eq. (16), then the  $\pi$ -pulse method offers a significant improvement in the fidelity, that is  $1 - \mathcal{F}' \ll 1 - \mathcal{F}$ .

The fidelity of diagonal unitary matrices is discussed in Appendix A. We will be interested in the case where  $\delta\Theta_{01} \simeq -\delta\Theta_{10} \gg \delta\Theta_{00}, \delta\Theta_{11}$ . In this case the fidelity of the phase gate without the  $\pi$  pulses is given by Eq. (19) and (A13) as

$$\mathcal{F} \simeq \cos^2 [(\delta\Theta_{01} - \delta\Theta_{10})/2], \quad (38)$$

while for the phase gate using the  $\pi$ -method Eq. (37) and (A10) give

$$\mathcal{F}' \simeq \cos^2(\delta\vartheta/2). \quad (39)$$

It should be recalled that each operation  $G$  is typically applied for half the time in the gate sequence (24) compared to the gate sequence (9). Therefore, the quantities  $\delta\Theta_{\alpha\beta}$  in Eq. (38) are not the same as the quantities  $\delta\Theta_{\alpha\beta}$  in Eq. (39) as the former are typically twice the size of the latter.

The  $\pi$ -pulse method (“spin-echo”) to suppress an unwanted term in a propagator (evolution operator) is one of the standard tools of NMR spectroscopy, which may be summarised as the observation that

$$[\sigma_x Z(\phi)]^2 = \sigma_x Z(\phi) Z(-\phi) \sigma_x = \mathbb{1}. \quad (40)$$

It relies on the assumption that the rotations  $Z$  in the error operator  $E$  in Eq. (21) are the same in two successive realisations of the gate operation  $G$  in the sequence (24). In the terminology of error correction, it takes advantage of a known correlation between two errors, thus giving an example of the fact that correlation in noise can be advantageous.

### F. Imperfect $\pi$ pulses

The  $\pi$ -pulse method can be a very helpful tool and it can strongly suppress the infidelity of a computational process. However, it assumes a cancellation of a large correlated error, which will only be exact when the correlated error terms are identical and the  $\pi$  pulses are perfect. Such a cancellation will in practice be sensitive to imprecisions in the  $\pi$  pulses and changes in the phases  $\Theta_{\alpha\beta}$ . We will next quantify this sensitivity.

The effect of a change in the phases  $\Theta_{\alpha\beta}$  between the two operations  $G$  in Eq. (24) can be absorbed into the imprecision of the  $\pi$  pulses. The imprecision in the  $\pi$  pulses can be modelled as a combination of error operators in the Pauli group. For instance, the imprecision in the duration of a  $\pi$  pulse will give an “over-rotation” error of the form

$$\begin{aligned} M &= \begin{bmatrix} \cos(\varepsilon/2) & -\sin(\varepsilon/2) \\ \sin(\varepsilon/2) & \cos(\varepsilon/2) \end{bmatrix} \\ &= \cos(\varepsilon/2) \mathbb{1} - i \sin(\varepsilon/2) \sigma_y, \end{aligned} \quad (41)$$

where  $\varepsilon$  is the imprecision in the angle through which the qubit is rotated in its Bloch sphere,  $\mathbb{1}$  is the unity operator and  $\sigma_y$  is the Pauli operator. More generally, the combination of the Pauli operators in the dynamics will depend on the character of noise in the system and may consist of (i) *unitary rotations* (which may or may not be factorisable into a pair of single-qubit rotations) or (ii) a *non-unitary relaxation*. All these cases can be treated by using appropriate superpositions or mixtures of the Pauli error operators. We analyse next examples of noise of both types.

### 1. Unitary rotations

It is convenient to consider a general unitary error in the  $\pi$  pulses as a combination of “over-rotations” in Eq. (41) and phase errors corresponding to rotations about the  $z$  axis of the Bloch sphere (see Eq. (5)).

First, we will consider pure phase errors. Let us suppose the first  $\pi$  pulse applied to ion  $j$  adds an additional rotation about the  $z$  axis by  $\tilde{\varepsilon}_j$ , and the second  $\pi$  pulse a rotation by  $p_j \tilde{\varepsilon}_j$ , where  $-1 \leq p_j \leq 1$ . To analyse the effects, we replace the two occurrences of  $R$  in Eq. (29) by  $R_1 R_2 Z_1(\tilde{\varepsilon}_1) Z_2(\tilde{\varepsilon}_2)$  and  $R_1 R_2 Z_1(p_1 \tilde{\varepsilon}_1) Z_2(p_2 \tilde{\varepsilon}_2)$ , respectively. Using the commutation and anticommutation properties as in Eq. (30)–(37), the fidelity of the phase gate with the imperfect  $\pi$  pulses is found to be

$$\begin{aligned} \tilde{\mathcal{F}} &= \left\langle \min |\langle \Psi_0 | Z_1[(1-p_1)\tilde{\varepsilon}_1] Z_2[(1-p_2)\tilde{\varepsilon}_2] E' | \Psi_0 \rangle|^2 \right\rangle \\ &\simeq \left\langle 1 - \mathcal{O}([\delta\vartheta + (1-p)\tilde{\varepsilon}]^2) \right\rangle. \end{aligned} \quad (42)$$

Next, consider pure “over-rotation” errors. To simplify the algebra we will assume both qubits have the same “over-rotation” angle, but the two different  $\pi$  pulses can have different “over-rotation” angles  $\varepsilon$  and  $p\varepsilon$ . Nothing essential is omitted by this simplification. It is found that

$$\tilde{\mathcal{F}} \simeq [1 - \mathcal{O}(\varepsilon^2)] \mathcal{F}', \quad (43)$$

in which the coefficient  $\varepsilon^2$  is of order  $1 + p^2$  and  $\mathcal{F}'$  is the fidelity of the phase gate with perfect  $\pi$  pulses (see Appendix B).

### 2. Non-unitary relaxation

The operator  $R$  in Eq. (22) represents perfect  $\pi$  pulses. Let us represent the imperfect  $\pi$  pulses with the following transformation

$$\mathcal{R}(\rho) = \sum_{\mu=1}^4 M_\mu \rho M_\mu^\dagger, \quad (44)$$

where  $\rho$  is the density operator describing the state of the qubits and  $M_\mu$  are Lindblad operators of the form

$$M_1 = \sqrt{(1-\zeta_1)(1-\zeta_2)} R_1 \otimes R_2, \quad (45a)$$

$$M_2 = \sqrt{(1-\zeta_1)\zeta_2} R_1 \otimes \mathbb{1}_2, \quad (45b)$$

$$M_3 = \sqrt{\zeta_1(1-\zeta_2)} \mathbb{1}_1 \otimes R_2, \quad (45c)$$

$$M_4 = \sqrt{\zeta_1\zeta_2} \mathbb{1}_1 \otimes \mathbb{1}_2, \quad (45d)$$

which satisfy the condition

$$\sum_{\mu=1}^4 M_\mu^\dagger M_\mu = \mathbb{1}. \quad (46)$$

The quantities  $\zeta_1$  and  $\zeta_2$  are bit-flip error probabilities for the qubit 1 and 2. In other words, the operator  $M_1$

represents the situation when both qubits are successfully flipped, the operator  $M_2$  ( $M_3$ ) corresponds to the failure to flip the qubit 2 (qubit 1) and finally the operator  $M_4$  stands for the failure to flip both qubits.

When using the non-unitary relaxation (44) to model errors due to the imperfect  $\pi$  pulses we describe a state of the qubits with a density operator. Then, the complete gate sequence reads

$$\begin{aligned}
\rho_0 &\xrightarrow{G} G\rho_0G^\dagger \\
&\xrightarrow{S} SG\rho_0G^\dagger S^\dagger \\
&\xrightarrow{\mathcal{R}} \mathcal{R}(SG\rho_0G^\dagger S^\dagger) \\
&\xrightarrow{G} G[\mathcal{R}(SG\rho_0G^\dagger S^\dagger)]G^\dagger \\
&\xrightarrow{\tilde{S}} \tilde{S}G[\mathcal{R}(SG\rho_0G^\dagger S^\dagger)]G^\dagger \tilde{S}^\dagger \\
&\xrightarrow{\mathcal{R}} \mathcal{R}(\tilde{S}G[\mathcal{R}(SG\rho_0G^\dagger S^\dagger)]G^\dagger \tilde{S}^\dagger),
\end{aligned} \tag{47}$$

where  $\rho_0 = |\Psi_0\rangle\langle\Psi_0|$  denotes an initial state of the qubits. The single-qubit rotations  $S$  are given by Eq. (3)–(4) with the replacement (8) and we introduced additional single-qubit rotations in the form

$$\tilde{S} = \tilde{S}_1 \otimes \tilde{S}_2 \tag{48}$$

with

$$\tilde{S}_1 = Z_1(\bar{\Theta}_{11} - \bar{\Theta}_{01}), \tag{49a}$$

$$\tilde{S}_2 = Z_2(\bar{\Theta}_{11} - \bar{\Theta}_{10}), \tag{49b}$$

where we dropped a global phase  $\bar{\Theta}_{01} + \bar{\Theta}_{10}$  in Eq. (47). The state of the qubits after the gate sequence (47) is derived in Appendix C.

The fidelity of the phase gate for an actual state described by a density operator is defined as

$$\tilde{\mathcal{F}} = \left\langle \min_{|\Psi_0\rangle} \langle \Psi_{\text{perf}} | \rho_{\text{act}} | \Psi_{\text{perf}} \rangle \right\rangle, \tag{50}$$

where  $|\Psi_{\text{perf}}\rangle$  denotes the perfect state (12), while  $\rho_{\text{act}}$  is the actual state (C3) after the gate sequence. The minimisation runs over all possible initial states  $|\Psi_0\rangle$ . Following Appendix C we obtain ( $\zeta \ll 1$ )

$$\tilde{\mathcal{F}} = (1 - 4\zeta)\mathcal{F}', \tag{51}$$

where  $\tilde{\mathcal{F}}$  is the fidelity of the phase gate with imperfect  $\pi$  pulses and  $\mathcal{F}'$  is the fidelity for perfect  $\pi$  pulses calculated in Eq. (28).

Note that the results (42), (43) and (51) all have a similar basic form, namely that the fidelity  $\tilde{\mathcal{F}}$  is the product of the fidelity  $\mathcal{F}'$  for perfect  $\pi$  pulses and a quantity which is approximately the fidelity of the  $\pi$  pulses themselves ( $\zeta \sim \varepsilon^2$ ). The essential point is that the system is not especially sensitive to imperfection in the  $\pi$  pulses, even though they are being used to cancel a large correlated error.

### III. IONS IN THE MICROTRAPS

In this section we shall introduce the proposal of Cirac and Zoller for the phase gate by pushing trapped ions in the microtraps [7, 8]. The basic principle is as follows. We consider two ions in two distinct harmonic potentials (so called *microtraps*) separated by a distance  $d \simeq 1 - 500\mu\text{m}$ . An internal-state-selective and time-dependent force is applied on both ions, such that each ion experiences the force when it is in an internal (logical) state  $|1\rangle$  and no force when it is in an internal (logical) state  $|0\rangle$  (FIG. 1).

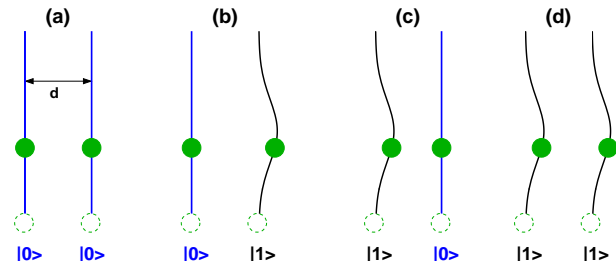


FIG. 1: The picture depicts trajectories of two ions corresponding to internal states  $|00\rangle, |01\rangle, |10\rangle, |11\rangle$ , where a time-dependent force applies on the ion only when it is in the internal state  $|1\rangle$ .

We assume that the pushing force is applied on a time scale much longer than an oscillation period of the ions in the microtraps (adiabatic approximation). We also consider the displacement of the ions  $\bar{x}$  due to the force to be small compared to the separation  $d$  between the microtraps ( $\bar{x} \ll d$ ). Then the Coulomb repulsion energy is given by

$$\begin{aligned}
E_{\text{coul}} &= \ell \left\{ \frac{1}{d}, \frac{1}{d + \bar{x}}, \frac{1}{d - \bar{x}}, \frac{1}{d} \right\} \\
&\approx \frac{\ell}{d} \left\{ 1, 1 - \frac{\bar{x}}{d} + \left(\frac{\bar{x}}{d}\right)^2, 1 + \frac{\bar{x}}{d} + \left(\frac{\bar{x}}{d}\right)^2, 1 \right\}
\end{aligned} \tag{52}$$

for the internal states  $\{|00\rangle, |01\rangle, |10\rangle, |11\rangle\}$ , where  $\ell = q^2/4\pi\epsilon_0$ . In this series expansion, the constant term produces a global phase. The term linear in  $\bar{x}$  produces single-qubit rotations, while the term quadratic in  $\bar{x}$  produces a two-qubit controlled-phase gate. If the force acts for time  $\tau$ , then a phase gate with a phase  $\vartheta$  expressed by Eq. (7) is obtained, where

$$\begin{aligned}
\vartheta &\sim -\frac{\ell}{\hbar} \int_0^\tau \left( \frac{1}{d} - \frac{1}{d + \bar{x}} - \frac{1}{d - \bar{x}} + \frac{1}{d} \right) dt \\
&\sim 2 \left( \frac{\bar{x}}{d} \right)^2 \frac{\ell\tau}{d\hbar},
\end{aligned} \tag{53}$$

The single-qubit rotations which are produced at the same time are rotations through some angles  $\phi$ , where

$$\phi \sim \frac{d}{\bar{x}} \vartheta. \tag{54}$$

More precise values of  $\vartheta$  and  $\phi$  will be obtained below.

The advantages of this gate are chiefly: (i) the gate time can be short, and (ii) it is found that when a finite temperature of the ions is taken into account, the dependence of the phases on the motional state of the ions is small when  $\bar{x} \ll d$ . However the condition  $\bar{x} \ll d$  implies that the linear term in the Taylor expansion is large compared to the quadratic term, and therefore when the gate time  $\tau$  is large enough to produce the desired phase  $\vartheta = \pi$  or  $\pi/2$ , the Coulomb repulsion produces a contribution to  $\phi$  which is large compared to  $\pi$  (typically  $\phi \sim 500\pi$ ). This means that the single-qubit phases are highly sensitive to small changes in the pushing force. Overall, a relative insensitivity to motional state is obtained at the price of sensitivity to fluctuations in the pushing force. In Sec. VI we discuss further methods (in addition to the  $\pi$ -pulse method) to reduce the influence of these fluctuations.

### A. Hamiltonian

The system of two ions trapped in two separate harmonic potentials (microtraps) with a time-dependent and internal-state-selective force applied on the ions is described in the semiclassical approach by the Hamiltonian

$$H(t) = \sum_{\alpha, \beta=0}^1 H_{\alpha\beta}(t) |\alpha\rangle_1 \langle\alpha| \otimes |\beta\rangle_2 \langle\beta|, \quad (55)$$

with

$$\begin{aligned} H_{\alpha\beta}(t) = & \frac{p_\alpha^2}{2m} + \frac{(p'_\beta)^2}{2m} \\ & + \frac{1}{2}m\omega^2(x_\alpha + d/2)^2 + \frac{1}{2}m\omega^2(x'_\beta - d/2)^2 \\ & + (s - x_\alpha - d/2)F_\alpha(t) + (s' - x'_\beta + d/2)F_\beta(t) \\ & + \frac{\ell}{|x'_\beta - x_\alpha|}, \end{aligned} \quad (56)$$

where the two bare microtraps with a trap frequency  $\omega$  are separated by a distance  $d$ ,  $m$  is the ion mass,  $x_\alpha(t)$  and  $x'_\beta(t)$  are coordinates (trajectories) of ions 1 and 2 corresponding to their internal states  $|\alpha = 0, 1\rangle_1$  and  $|\beta = 0, 1\rangle_2$ ,  $p_\alpha(t)$  and  $p'_\beta(t)$  are momenta of the ions. We denoted  $\ell = q/4\pi\epsilon_0$ , where  $q$  is the ion charge and  $\epsilon_0$  is the permittivity of vacuum. The parameters  $s$  and  $s'$  are associated with the potential which the ions experience when they are in their equilibrium positions ( $x = \pm d/2$ ) in the microtraps. The quantity  $F_\alpha(t)$  denotes an internal-state-selective and time-dependent force which displaces the ion only when it is in its internal (logical) state  $|1\rangle$ . We shall consider the force in the form

$$F_\alpha(t) = \alpha\hbar\omega f(t)/a, \quad (57)$$

where  $\alpha = 0, 1$  refers to the internal ionic state  $|0\rangle$  and  $|1\rangle$ ,  $f(t)$  is a dimensionless time profile and we define

$$a = \sqrt{\frac{\hbar}{m\omega}}. \quad (58)$$

The quantity  $a$  is equal (up to the factor  $1/\sqrt{2}$ ) to the ground state width of a quantum harmonic oscillator. In this and subsequent sections it is assumed that the force depends on time but not on position. The effect of a dependence on position is then discussed in Sec. VII.

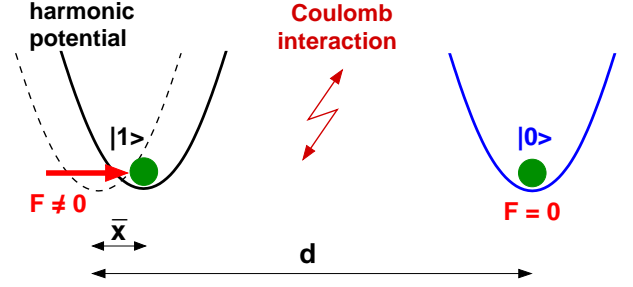


FIG. 2: Two ions (representing two qubits) are trapped in two distinct harmonic potentials separated by a distance  $d$ . A state-selective force displaces the trapping potential of the ion only when it is in the logical state  $|1\rangle$ .

The coordinates  $x_\alpha$  and  $x'_\beta$  describe positions of the ions with respect to the centre-of-mass of the system. It is convenient to apply a transformation

$$x_\alpha \rightarrow x_\alpha - d/2, \quad (59a)$$

$$x'_\beta \rightarrow x'_\beta + d/2, \quad (59b)$$

where new coordinates refer rather to the equilibrium positions of the ions in the microtraps. When we use the transformation (59), the Hamiltonian (56) can be rewritten in the form

$$\begin{aligned} H_{\alpha\beta}(t) = & \frac{p_\alpha^2}{2m} + \frac{(p'_\beta)^2}{2m} \\ & + \frac{1}{2}m\omega^2 [(x_\alpha - \bar{x}_\alpha)^2 - \bar{x}_\alpha^2 + 2\bar{x}_\alpha s] \\ & + \frac{1}{2}m\omega^2 [(x'_\beta - \bar{x}'_\beta)^2 - (\bar{x}'_\beta)^2 + 2\bar{x}'_\beta s'] \\ & + \frac{\ell}{|d + x'_\beta - x_\alpha|}, \end{aligned} \quad (60)$$

where we introduced

$$\bar{x}_\alpha(t) = F_\alpha(t)/m\omega^2 = \alpha a f(t), \quad (61a)$$

$$\bar{x}'_\beta(t) = F_\beta(t)/m\omega^2 = \beta a f(t). \quad (61b)$$

In Eq. (60) the action of the force can be interpreted as a displacement of the potential in which each ion is trapped and this displacement takes place only when the ion is in its internal state  $|1\rangle$ . The distance scale of the displacements is given by the quantity  $a$  defined in Eq. (58).

## B. Dynamics

The dynamics of the ion system is governed by the evolution operator

$$U = D \exp \left[ -\frac{i}{\hbar} \int_{t_0}^t H(t') dt' \right], \quad (62)$$

where the Hamiltonian is given by Eq. (55) and  $D$  is the Dyson time-ordering operator. It follows from Eq. (55) and (62) that

$$U|\alpha\beta\rangle = e^{i\Theta_{\alpha\beta}}|\alpha\beta\rangle, \quad (63)$$

where

$$\Theta_{\alpha\beta} = -\frac{1}{\hbar} \int_{t_0}^t H_{\alpha\beta}(t') dt'. \quad (64)$$

Thus, the dynamics of the ion system described by the Hamiltonian (56) corresponds to a rotation of the joint internal state of the ions  $|\alpha\beta\rangle$  by *dynamical phases*  $\Theta_{\alpha\beta}$ . In Sec. IV we shall analyse the phases  $\Theta_{\alpha\beta}$  in order to apply them in the general discussion of Sec. II. However, first we have to understand the motion of the ions in the microtraps.

## C. Motion of the ions

Once we understand the motion of a single ion in a microtrap with an external pushing force, it is relatively simple to generalise its behaviour to two ions because the presence of a second ion in a separate microtrap causes via the Coulomb interaction only small perturbations (under a certain approximation) to the motion of the first ion and vice versa.

The motion of a single trapped ion is discussed in Appendix D and it appears that it consists of three different motions. We see from Eq. (D7) that the sloshing motion is a fast transitory motion depending on the turn-on rate of the force ( $\dot{x} \propto \dot{F}$ ). In other words, when we turn on the force sufficiently slowly compared to oscillations of the ion, the contribution of the sloshing part to the overall motion will be negligible. Then, we refer to so called *adiabatic approximation*. When we assume the displacement of the potential and oscillations of the ion to be of the same order ( $\bar{x} \sim \Delta$ ), then the adiabatic approximation can be estimated from the condition  $|\delta x| \ll \min\{\bar{x}, \Delta\}$  as follows

$$\left| \int_{t_0}^t \dot{f}(t') e^{i\omega t'} dt' \right| \ll f(t), \quad (65)$$

where  $\dot{f} = df/dt$ . For a Gaussian time profile of the force

$$f(t) = \xi e^{-(t/\tau)^2}, \quad (66)$$

the adiabatic approximation (65) requires

$$e^{-(\omega\tau/2)^2} \ll 1 \quad \Rightarrow \quad \omega\tau \gg 1. \quad (67)$$

This means that the time scale  $\tau$  on which the force applies has to be much longer than the oscillation period  $T_{\text{osc}} = 2\pi/\omega$  of the ion. The duration of the force  $\tau$  and the dimensionless amplitude  $\xi$  in Eq. (66) are quantities which characterise the force. They have to be chosen such that the adiabatic condition (67) and the phase condition ( $\bar{\vartheta} = \pi$  or  $2\bar{\vartheta} = \pi$ ) are satisfied. In the adiabatic approximation the motion of the ion which is in the internal state  $|\alpha\rangle$  simplifies to the form

$$x_\alpha(t) \approx \bar{x}_\alpha(t) + \Delta(t), \quad (68)$$

where the displacement  $\bar{x}_\alpha(t)$  is defined in Eq. (61) and the oscillations  $\Delta(t)$  are given by Eq. (D9).

Now let us consider the case of two ions in two separate identical traps. The Coulomb repulsion between the ions affects their separation. When two bare microtraps (i.e. microtraps without the ions) are separated by a distance  $d$ , then the equilibrium distance between two ions loaded into the microtraps is bigger by the amount

$$\Delta d = \frac{4d}{3} \sinh^2 \left\{ \frac{1}{6} \ln \left[ \eta + 1 + \sqrt{\eta(\eta + 2)} \right] \right\}, \quad (69)$$

where  $\eta = 27\epsilon/4$  and

$$\epsilon \equiv \frac{q^2}{\pi\epsilon_0 m\omega^2 d^3} \quad (70)$$

gives the ratio between the Coulomb energy and the trapping energy. For  $\epsilon \ll 1$  the expression in Eq. (69) simplifies to  $\Delta d \approx \epsilon d/2$  but we will be also interested in the case when  $\epsilon \lesssim 1$ .

The presence of a second ion also causes a shift in the oscillation frequency of the first ion and vice versa. In a 3D treatment [8] and taking into account up to the quadratic term in the Coulomb energy, the oscillation frequency in the longitudinal direction is corrected by the factor

$$\omega_{\text{osc}}/\omega_{\text{trap}} = \sqrt{1 + \epsilon}, \quad (71)$$

with a factor  $\sqrt{1 - \epsilon/2}$  for the transversal oscillation frequency. The higher order Coulomb terms cause the net potential at each ion to be anharmonic and we will retain the third and fourth order in the discussion to follow. However, in order to keep the expressions uncluttered, we will ignore the distinction between  $\omega_{\text{osc}}$  and  $\omega_{\text{trap}}$ . In any case, a fully accurate consideration of this point requires a fully quantum treatment [8] of the motion rather than the semiclassical one adopted here.

## IV. DYNAMICAL PHASES

Now we are able to analyse in detail the dynamical phases  $\Theta_{\alpha\beta}$  in Eq. (64) which have a key importance in the quantum phase gate because they correspond to the phases in Eq. (6). We will assume



- (i) Adiabatic approximation – given by Eq. (67) for the Gaussian time profile of the force:  $\omega\tau \gg 1$ .
- (ii) Displacements of the potentials and oscillations of the ions are small compared to the trap separation:  $\bar{x}, \Delta \ll d$  (weak force, low temperature).
- (iii) Tight trapping potentials with respect to the Coulomb repulsion:  $\epsilon \lesssim 1$ .

Regarding the third assumption, the analysis simplifies in the limit  $\epsilon \ll 1$ , and owing to this some of the analytical results to be discussed will only be precise in that limit. Namely,  $\epsilon \ll 1$  allows us to assume the harmonicity of the potential what we used in Appendix D. However, the gate can still operate with high fidelity when  $\epsilon \sim 1$ .

When we now substitute Eq. (60) into Eq. (64) we find that we deal with *single-particle* and *two-particle* phases. Therefore, we write the phases  $\Theta_{\alpha\beta}$  in the form

$$\Theta_{\alpha\beta} = \varphi_\alpha + \varphi'_\beta + \phi_\alpha + \phi'_\beta + \phi_{\alpha\beta}, \quad (72)$$

where  $\alpha, \beta = 0, 1$  and we introduce so called *kinetic phases*

$$\varphi_\alpha = -\frac{1}{\hbar} \int_{t_0}^t \frac{p_\alpha^2}{2m} dt', \quad (73a)$$

$$\varphi'_\beta = -\frac{1}{\hbar} \int_{t_0}^t \frac{(p'_\beta)^2}{2m} dt', \quad (73b)$$

then the single-particle phases due to the trapping potential and the force

$$\phi_\alpha = -\frac{1}{\hbar} \int_{t_0}^t \frac{1}{2} m \omega^2 [(x_\alpha - \bar{x}_\alpha)^2 - \bar{x}_\alpha^2 + 2\bar{x}_\alpha s] dt', \quad (74a)$$

$$\phi'_\beta = -\frac{1}{\hbar} \int_{t_0}^t \frac{1}{2} m \omega^2 [(x'_\beta - \bar{x}'_\beta)^2 - (\bar{x}'_\beta)^2 + 2\bar{x}'_\beta s'] dt', \quad (74b)$$

and finally the two-particle phases originating from the Coulomb interaction between the ions

$$\phi_{\alpha\beta} = -\frac{1}{\hbar} \int_{t_0}^t \frac{\ell}{|d + x'_\beta - x_\alpha|} dt'. \quad (75)$$

We will assume that  $t_0 < 0$ ,  $t > 0$  and  $|t|, |t_0| \gg \tau$ , where  $\tau$  is the gate time.

### A. Kinetic phases

The kinetic phases in Eq. (73) are associated with the kinetic energy of the ions. We can calculate them using the expression for the motion of the ions in Eq. (68). Taking into account that  $p = m\dot{x}$  and assuming that  $|t_0|, |t| \rightarrow \infty$  (it means that we turn the force gradually

on from the zero value and turn it slowly off back to the zero) we can write

$$\begin{aligned} \varphi_\alpha &= -\frac{m}{2\hbar} \int_{-\infty}^{+\infty} \left( \dot{\bar{x}}_\alpha^2 + 2\dot{\bar{x}}_\alpha \dot{\Delta} + \dot{\Delta}^2 \right) dt \\ &= \varphi_\alpha^I + \varphi_\alpha^{II} + \varphi_\alpha^{III}. \end{aligned} \quad (76)$$

For the Gaussian time profile (66) we get

$$\varphi_\alpha^I = -\frac{\alpha^2 \xi^2}{\omega\tau} \sqrt{\frac{\pi}{8}} \quad (77)$$

and

$$\varphi_\alpha^{II} = -\alpha\omega\tau\xi e^{-(\omega\tau/\sqrt{2})^2} \sqrt{\frac{2\pi\mathcal{E}}{\hbar\omega}} \cos\psi, \quad (78)$$

where  $\alpha = 0, 1$  correspond to the internal states  $|0\rangle$  and  $|1\rangle$ ,  $\xi$  and  $\tau$  are defined in Eq. (66) and  $\mathcal{E}$  with  $\psi$  are introduced in Eq. (D9). The contribution  $\varphi_\alpha^{III}$  in Eq. (76) is a global phase which does not depend on the internal state  $|\alpha\rangle$  and can be omitted.

The displacement  $\bar{x}$  scales with the quantity  $a$  introduced in Eq. (58), and by assumption (ii) it is much smaller than the ion separation  $d$ . Therefore, it is reasonable to assume that the parameter  $\xi$  in Eq. (61) is of the order of one or smaller ( $\xi \lesssim 1$ ). Then, it follows from Eq. (77) and (78) that  $\varphi_\alpha^I < \pi$ , or  $\varphi_\alpha^I \ll \pi$  when the adiabatic condition is very well obeyed.

The contribution  $\varphi_\alpha^{II}$  vanishes very rapidly with the adiabatic approximation (67). Outside the adiabatic regime the phase  $\varphi_\alpha^{II}$  would be responsible for a sensitivity of the gate to the motional state because  $\varphi_\alpha^{II}$  scales with  $\sqrt{\mathcal{E}}$ , where  $\mathcal{E}$  is the oscillation energy of the ion. In the full quantum approach we would find that the phase contribution  $\varphi_\alpha^{II}$  corresponds to entanglement between motional and internal degrees of freedom of the ions which spoils the performance of the gate.

### B. Single-particle potential energy phases

The phases in Eq. (74) are associated with the trapping potential energy and energy introduced to the system via the external force  $F$ . When we substitute Eq. (68) into Eq. (74) we obtain

$$\phi_\alpha = \sqrt{\frac{\pi}{8}} \alpha\omega\tau\xi^2 - \sqrt{\pi} \alpha\omega\tau\xi \frac{s}{a}, \quad (79)$$

where  $\alpha = 0, 1$  and we omitted the first term in Eq. (74) because it contributes only a global phase. With assumptions (i) and (ii), where  $\bar{x} \sim a$ , we find  $\phi_\alpha \gg \pi$ . We obtain the expression for  $\phi'_\beta$  when we replace  $\alpha$  with  $\beta$  and  $s$  with  $s'$  in Eq. (79).

### C. Two-particle interaction phases

Finally, we can analyse the two-particle interaction phases in Eq. (75). They have a key importance in the scheme of the phase gate because they actually produce the phase  $\vartheta$  in Eq. (6). The phases  $\phi_{\alpha\beta}$  are highly nonlinear but we can expand them in a Taylor series using assumption (ii). Then we can rewrite Eq. (75) in the form

$$\phi_{\alpha\beta} = -\frac{\ell}{\hbar d} \int_{t_0}^t \sum_{n=0}^{\infty} \left( \frac{x_{\alpha} - x'_{\beta}}{d} \right)^n dt', \quad (80)$$

where  $\phi_{\alpha\beta}$  are calculated with precision up to  $n = 4$  in Appendix E. The term of order  $n = 0$  contributes only with a global phase and can be omitted. The linear term ( $n = 1$ ) in Eq. (E6) has a character of a single-qubit phase and it is the quadratic term ( $n = 2$ ) in Eq. (E8) which finally produces a two-particle interaction between the ions via the Coulomb repulsion. We consider also higher order terms with  $n = 3$  and  $n = 4$  in Eq. (E9) and (E10) because they contribute with thermal motion contributions. In principle it would be sufficient to take into account only the cubic term ( $n = 3$ ) but with the help of the  $\pi$ -pulse method we are able to undo contributions of the odd terms. Therefore, we have to consider also the bi-quadratic term ( $n = 4$ ) as a lowest order correction to the quadratic term when we apply the  $\pi$ -pulse method.

Using the results from Appendix E we can calculate the phase  $\vartheta$  defined by Eq. (7). That is

$$\begin{aligned} \vartheta &= \Theta_{11} - \Theta_{10} - \Theta_{01} + \Theta_{00} \\ &= \phi_{11} - \phi_{10} - \phi_{01} + \phi_{00} \\ &= \theta \left\{ 1 + \left( \frac{a}{d} \right)^2 \times \right. \\ &\quad \left. \times \left[ \frac{\xi^2}{\sqrt{2}} + 6 \left( \frac{E_1}{\hbar\omega} + \frac{E_2}{\hbar\omega} - 2 \frac{\sqrt{E_1 E_2}}{\hbar\omega} \cos(\Delta\psi) \right) \right] \right\}, \end{aligned} \quad (81)$$

where all single-particle phases  $\varphi_{\alpha}$ ,  $\varphi'_{\beta}$ ,  $\phi_{\alpha}$ ,  $\phi'_{\beta}$  cancelled out and only the two-particle phases  $\phi_{\alpha\beta}$  contributed,  $\Delta\psi = \psi_1 - \psi_2$  and we introduced the quantity

$$\theta \equiv \sqrt{\frac{\pi}{8}} \epsilon \omega \tau \xi^2. \quad (82)$$

It follows from assumption (i) that  $\omega\tau \gg 1$ , from assumption (iii) that  $\epsilon \lesssim 1$  and we aim for the phase gate with  $\vartheta = \pi$  or  $2\vartheta = \pi$ . Therefore, we confirm that  $\xi \lesssim 1$  as we assumed previously in the discussion after Eq. (78).

In order to calculate the fidelity of the phase gate with ions in the microtraps we need to express the quantity  $\delta\Theta_{\alpha\beta}$  in Eq. (18). However, first we need to make a good estimate for the phases  $\Theta_{\alpha\beta}$  in Eq. (8).

After laser cooling we can describe the oscillation motion of the ions with the Boltzmann thermal distribution with the probability

$$p(\mathcal{E}) = \frac{1}{Z} e^{-\mathcal{E}/k_B T}, \quad (83)$$

where  $k_B$  is the Boltzmann constant,  $T$  is the temperature and  $\mathcal{E}$  is the oscillation energy of the ion. Further, it seems to be realistic to describe the oscillation phases  $\psi_1$  and  $\psi_2$  in Eq. (E4) with a uniform distribution. Then, a good estimate for the phases  $\bar{\Theta}_{\alpha\beta}$  is the average value

$$\bar{\Theta}_{\alpha\beta} \equiv \int_0^{2\pi} \frac{d\psi_1 d\psi_2}{(2\pi)^2} \int_0^{+\infty} \frac{d\mathcal{E}_1 d\mathcal{E}_2}{(k_B T)^2} \Theta_{\alpha\beta} e^{-(\mathcal{E}_1 + \mathcal{E}_2)/k_B T}. \quad (84)$$

Taking the case that fluctuations in the pushing force are negligible, the parameter  $\xi$  has a fixed value during the gate operation. Then, we can write

$$\delta\Theta_{\alpha\beta} = \Theta_{\alpha\beta} - \bar{\Theta}_{\alpha\beta} = \phi_{\alpha\beta} - \bar{\phi}_{\alpha\beta}, \quad (85)$$

and the gate phase in Eq. (10) is

$$\bar{\vartheta} = \theta \left[ 1 + \left( \frac{a}{d} \right)^2 \left( \frac{\xi^2}{\sqrt{2}} + \frac{12k_B T}{\hbar\omega} \right) \right], \quad (86)$$

where we used Eq. (E12). We require  $\bar{\vartheta} = \pi$  or  $2\bar{\vartheta} = \pi$  to realise the phase gate and it follows from assumption (ii) that  $a \ll d$  (because  $\xi \lesssim 1$ ). Therefore, the phase condition reduces to  $\theta \approx \pi$  or  $2\theta \approx \pi$ . It follows from Eq. (82) that the phase condition determines directly the *gate time*  $\tau$  (for given values of the other parameters).

Finally, we can calculate the fidelity of the phase gate without the  $\pi$  pulses given by the sequence (6). When we substitute Eq. (E11) and (E12) into Eq. (20) we get

$$\mathcal{F} = 1 - \left( \frac{6\theta k_B T}{\hbar\omega} \right)^2 \left[ \frac{1}{\xi^2} \left( \frac{a}{d} \right)^2 - 2 \left( \frac{a}{d} \right)^4 \right], \quad (87)$$

where the minimisation is carried out in the original paper [8] and this result corresponds also to Eq. (38). The fidelity of the phase gate with perfect  $\pi$  pulses defined by Eq. (28) and corresponding to the sequence (24) is

$$\mathcal{F}' = 1 - \left( \frac{6\theta k_B T}{\hbar\omega} \right)^2 \left( \frac{a}{d} \right)^4, \quad (88)$$

corresponding to Eq. (39). Comparing Eq. (87) and (88) it is seen that the  $\pi$ -pulse method improves the fidelity by two orders in  $a/d$ , and we will see later that  $a/d \sim 10^{-3}$ .

## V. PUSHING FORCE

The state-dependent force was introduced in Eq. (56) and Eq. (57), but we have not yet specified how it can be realised in practice. In this section we discuss the dipole force (originating from a laser beam) as a suitable candidate force. We will consider the dipole force in a travelling-wave and a standing-wave configuration. The dipole force is always associated with some unwanted photon scattering which reduces the fidelity of the gate. Quantifying this is the main aim of this section.

### A. Dipole force

The *dipole force* is produced in an intensity gradient of the light illuminating the atom, typically a laser beam which is far detuned from some atomic transition. The relevant atomic levels are light-shifted (AC Stark shift) creating an additional potential for the particle. When the laser is tuned below the atomic frequency (red detuning), the particle is driven towards the laser intensity maximum, i.e. to the minimum of the created potential (FIG. 3). For a blue detuning the particle is pushed away from the intensity maximum.

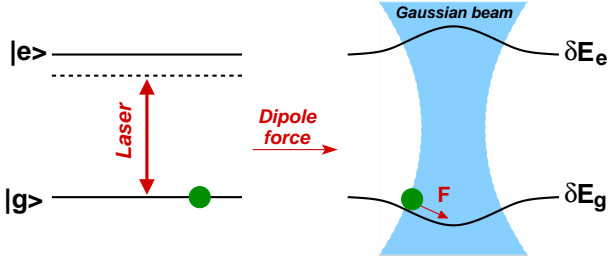


FIG. 3: Non-resonant laser beam causes AC Stark light shifts with a magnitude dependent on the intensity profile of the laser beam. The light shifts produce a dipole force which pushes the atomic particle towards the minimum of the laser-light potential.

Let us assume a two-level atom (ion) with a lower level  $|g\rangle$  and an upper level  $|e\rangle$  separated by an atomic frequency  $\omega_A$ . The  $|g\rangle$  state corresponds to the logical state  $|1\rangle$  of the ion while the  $|e\rangle$  state is an excited auxiliary state. The logical state  $|0\rangle$  is not to be coupled to the light (FIG. 4). When we apply a laser beam of frequency  $\omega_L$  the atom-laser Hamiltonian in the dipole approximation is

$$H = \frac{\hbar\omega_0}{2}\sigma_z + \frac{\hbar\Omega}{2}(\sigma_+ + \sigma_-) \left[ e^{i(\omega_L t + \phi_L)} + e^{-i(\omega_L t + \phi_L)} \right], \quad (89)$$

where  $\sigma_z = |e\rangle\langle e| - |g\rangle\langle g|$ ,  $\sigma_+ = |e\rangle\langle g|$ ,  $\sigma_- = |g\rangle\langle e|$ ,  $\Omega(\mathbf{r}, t)$  is the Rabi frequency on the transition  $|e\rangle \leftrightarrow |g\rangle$  and we assumed the laser can be treated as a classical light field. In the limit of large detuning  $\Delta = \omega_L - \omega_A \gg |\Omega|$ , the standard treatment of this “two-level atom” leads to the dipole force (on the atom in the  $|g\rangle$  state)

$$\mathbf{F}_{\text{dip}} = -\frac{\hbar}{4\Delta} \nabla |\Omega(\mathbf{r})|^2. \quad (90)$$

In the *travelling-wave configuration* we place the ion off the axis of the laser beam and use its non-uniform intensity profile

$$\Omega_{\text{trav}} = \Omega_0 e^{-(t/\tau\sqrt{2})^2} e^{-[(x-x_0)/w]^2} e^{ikz}, \quad (91)$$

where  $x - x_0$  refers to the position of the ion in the profile (cross-section) of the laser beam. We assumed the exponential time profile of the laser pulse with a duration  $\tau$  and the Gaussian intensity profile with the size

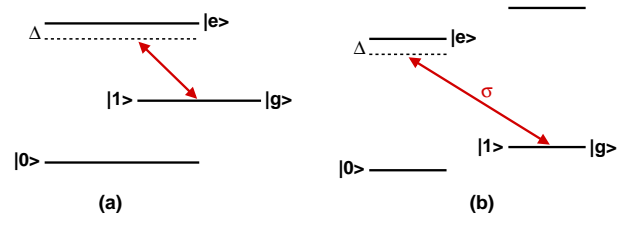


FIG. 4: (a) Logical states  $|0\rangle$  and  $|1\rangle$  of the ion qubit are represented by a ground and excited (metastable) atomic (ionic) levels. A non-resonant laser does not couple the state  $|0\rangle$ . (b) Logical states are represented by two sublevels of a ground state manifold. Coupling of the  $|0\rangle$  state is prevented by polarization selection rules, for example using a  $\sigma$ -polarized laser.

of the beam waist  $w$  and the radial distance  $x$ . We also introduced the constant

$$|\Omega_0|^2 = \frac{6\pi\Gamma I}{\hbar ck^3} = \frac{12\Gamma P}{\hbar ck^3 w^2}, \quad (92)$$

where  $\Gamma$  is the line width of the  $|g\rangle \rightarrow |e\rangle$  transition,  $I$  and  $P$  are the intensity and power of the laser,  $c$  is the speed of light and  $k = 2\pi/\lambda$  is the wave number with the laser wavelength  $\lambda$ .

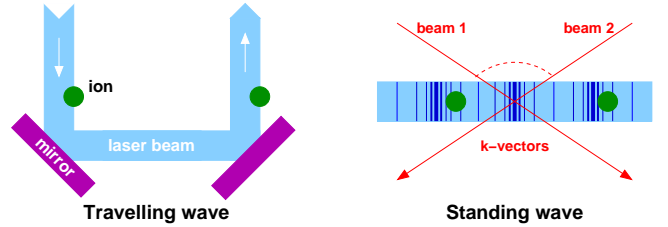


FIG. 5: Scheme of the travelling-wave and the standing-wave configuration. The travelling wave is created by a single laser beam deflected by mirrors. The standing wave is created by two laser beams with different  $k$ -vectors. By adjusting the angle between the  $k$ -vectors the period of the standing wave (node-antinode separation) can be changed.

In the *standing-wave configuration* we rather use the gradient of the standing field of the laser, giving

$$\Omega_{\text{stan}} = 2i\Omega_0 e^{-(t/\tau\sqrt{2})^2} e^{-(x/w)^2} \sin[k(z - z_0)], \quad (93)$$

where  $z - z_0$  corresponds to the position of the ion in the standing-wave field. When we now substitute Eq. (92) and (93) into Eq. (90) we calculate the pushing dipole force on the ions. Comparing the expression of the dipole force (90) with the general form of the pushing force in Eq. (57) we can express the dimensionless amplitude  $\xi$ , giving

$$\xi_{\text{trav}} = \frac{a(x - x_0)}{\omega\Delta w^2} |\Omega_0|^2 e^{-2[(x-x_0)/w]^2}, \quad (94a)$$

$$\xi_{\text{stan}} = -\frac{ak}{\omega\Delta} |\Omega_0|^2 \sin[2k(z - z_0)] e^{-2(x/w)^2}. \quad (94b)$$

It follows from Eq. (94) that the maximum force is for  $x_0 = w/2$  in the travelling-wave and for  $kz_0 = \pi/4$  in the standing-wave configuration.

## B. Photon scattering

We use a far detuned laser to create a dipole pushing force on the ions. Even though the laser is far detuned from the  $|g\rangle \leftrightarrow |e\rangle$  transition there is still some photon scattering due to a non-zero line width  $\Gamma$  of the transition. A single scattered photon is sufficient to destroy the fidelity of the gate, because scattering only takes place in the qubit logical state  $|1\rangle$ , not in the logical state  $|0\rangle$ . Therefore, a scattering event constitutes a measurement of the qubit by the environment. We have to choose parameters so that the number of photons scattered during the gate is small compared to one ( $N \ll 1$ ).

The *scattering rate* in the two-level atom approximation and in the weak-coupling regime ( $|\Omega|, \Gamma \ll |\Delta|$ ) is [10]

$$R = \frac{\Gamma}{2} \frac{|\Omega|^2/2}{\Delta^2 + (\Gamma/2)^2 + |\Omega|^2/2} \approx \frac{\Gamma}{4} \frac{|\Omega|^2}{\Delta^2}. \quad (95)$$

The *number of scattered photons* during the gate operation, i.e. during the period when the laser is on and drives the  $|g\rangle \leftrightarrow |e\rangle$  transition, is given by

$$N = \int_{t_0}^t R(t') dt', \quad (96)$$

where we assume that the laser is gradually switched on and off as stated in Eq. (91) and (93), and the comment below Eq. (75) applies. When we now substitute for the coupling constant  $\Omega$  the number of scattered photons can be expressed in the travelling-wave configuration as

$$N_{\text{trav}} \approx C_{\text{trav}} \frac{w^6 d^3 \omega^4}{x_0^2 P} e^{2(x_0/w)^2} \quad (97)$$

and in the standing-wave configuration as

$$N_{\text{stan}} \approx C_{\text{stan}} w^2 \frac{d^3 \omega^4}{P} \frac{1}{\cos^2(kz_0)}, \quad (98)$$

where the constants are

$$C_{\text{trav}} = \left( \frac{\pi^5 \sqrt{2} \varepsilon_0 c}{3 q^2} \right) \frac{m^2}{\lambda^3}, \quad (99a)$$

$$C_{\text{stan}} = \left( \frac{\pi^3 \sqrt{2} \varepsilon_0 c}{12 q^2} \right) \frac{m^2}{\lambda}, \quad (99b)$$

and we assumed that the distance moved by the ion was small compared to the waist size  $w$  (period  $\pi/k$ ) in the travelling-wave (standing-wave) configuration.

To calculate the number of scattered photons in Eq. (97) and (98) we also needed to express the gate time

$\tau$  from Eq. (82), where the phase condition for the gate with the  $\pi$  pulses has to be satisfied. It follows from Eq. (86) that  $2\theta \approx \pi$ , giving

$$\tau = \frac{\sqrt{2\pi}}{\varepsilon \omega \xi^2}, \quad (100)$$

and we use the expression in Eq. (94) for the parameter  $\xi$ . We also took into account that we apply two successive gate pulses.

When we compare photon scattering for the travelling-wave and the standing-wave configuration we get (assuming  $x_0 \sim w$ )

$$\frac{N_{\text{trav}}}{N_{\text{stan}}} \sim \left( \frac{w}{\lambda} \right)^2, \quad (101)$$

where  $w$  is the size of the laser beam waist and  $\lambda$  is the wavelength of the laser light. In practice, we shall have  $w \sim 10^{-6}$  m and  $\lambda \sim 10^{-7}$  m, that is  $N_{\text{trav}}/N_{\text{stan}} \sim 100$ . This means that in the travelling-wave configuration we have approximately 100-times more photon scattering. This is because for a given laser intensity, the smaller intensity gradient of the travelling wave (compared to the gradient of the standing wave) leads to a smaller force, hence a longer gate time and more scattered photons. Alternatively, if the force is increased for the travelling wave case by reducing the detuning, the scattering rate goes up as  $1/\Delta^2$  and hence again there are more scattered photons.

The travelling-wave configuration nevertheless has an advantage. The ions oscillate in the microtraps due to non-zero temperature and experience different instant magnitudes of the force in different points within the laser beam. In the travelling-wave configuration the excursion of the ion thermal motion  $\Delta_{\text{osc}}$  is limited approximately by  $\Delta_{\text{osc}} \ll w$ , while in the standing-wave configuration it has the stronger constraint  $\Delta_{\text{osc}} \ll \lambda$  (Lamb-Dicke regime). Therefore, the latter case requires more laser cooling and it is generally more experimentally demanding.

## C. Contribution of scattering to the infidelity

We have already discussed in Sec. VB that photon scattering appears only when the ion is in the logical state  $|1\rangle$  and therefore constitutes a measurement of the qubit. A measurement will cause a state reduction such that fidelity falls to 1/2 in the worst case. However, depending on the atomic structure, photon scattering might also be associated with optical pumping of the state from the state  $|1\rangle$  to  $|0\rangle$ , in which case a single scattered photon can reduce the fidelity to zero in the worst case. Making the latter (i.e. more cautious) assumption, we therefore estimate the influence of photon scattering on the fidelity as

$$\mathcal{F}_{\text{scat}} = e^{-N} \approx 1 - N, \quad (102)$$

where  $N$  is the overall number of scattered photons during the phase gate and it only makes sense to consider  $N \ll 1$ . The number  $N$  is given by Eq. (97) and (98) depending on the experimental realisation.

## VI. INFLUENCE OF FLUCTUATIONS

### A. Fluctuations in single-qubit phases

In the original work [8] the single-particle phases were regarded as not contributing to loss of fidelity, by the argument that as long as their value is known, the correct single-qubit rotation operator can be applied to a very good precision. However, as we commented in Sec. IV, there are present some very large terms in the single-qubit phases, so that even a small relative change in the value of a parameter may introduce an unknown phase change of the order of  $\pi$  and completely destroy the fidelity. For example, when the force is provided by a laser beam as discussed in Sec. V, intensity fluctuations of the laser cause fluctuations in the pushing force  $F$  and therefore in its amplitude  $\xi$ . The single-qubit phases are highly sensitive to such changes when  $a \ll d$  (or more precisely  $a\xi \ll d$ ).

Bringing together Eq. (72), (77), (79) and (E12) we obtain the phase required for the single-qubit operation  $S_1$  in Eq. (4), giving

$$\begin{aligned} \Phi_1 &\equiv \bar{\Theta}_{10} - \bar{\Theta}_{00} \\ &= \theta \left[ -\frac{1}{\epsilon(\omega\tau)^2} + \frac{1}{\epsilon} - \frac{s\sqrt{8}}{a\xi\epsilon} - \frac{d}{a} \frac{1}{\xi\sqrt{2}} - \frac{1}{2} + \mathcal{O}(a/d) \right], \end{aligned} \quad (103)$$

where the first term corresponds to the kinetic phase  $\varphi_\alpha^I$  in Eq. (77) and we dropped  $\varphi_\alpha^II$  since it is strongly suppressed in the adiabatic limit. The second and the third term come from the potential energy phase in Eq. (79) and they correspond to the *light shift phases* because the pushing force is represented by the dipole force. The next two terms correspond to the linear and quadratic contribution from the Taylor expansion of the Coulomb energy and  $\mathcal{O}(a/d)$  denotes higher order terms in this expansion.

The expression for  $\Phi_2 \equiv \bar{\Theta}_{01} - \bar{\Theta}_{00}$  is the same as  $\Phi_1$  in Eq. (103) except  $s$  is replaced by  $s'$  and the odd-order Coulomb terms in  $d/a$  and  $a/d$  change sign. Further, we will discuss the case when  $\Phi_j$  can be different in two successive gate operations  $G$  in the sequence (24) due to the influence of fluctuations of experimental parameters.

The  $\pi$ -pulse method goes some way towards alleviating the effects of these fluctuations, since then the overall sequence is only sensitive to a change in the single-qubit phases between the two successive applications of the gate operation  $G$ . Let these two successive pushing gates be  $G_1$  and  $G_2$ , so the gate sequence for the phase gate with the  $\pi$  pulses is  $S'(RG_2)(RG_1)$ . Using Eq. (15)

we define error operators

$$E_j \equiv G_j G_{\text{perf}}^\dagger, \quad (104)$$

where  $j = 1, 2$ . Then, the gate sequence is

$$S'(RG_2)(RG_1) \rightarrow S'[R(E_2 G_{\text{perf}})] [R(E_1 G_{\text{perf}})]. \quad (105)$$

Without loss of generality, the error operator  $E_1$  may be taken equal to  $E$  in Eq. (21) and we write  $E_2$  in the form

$$E_2 = Z_1(\Delta\Phi_1) Z_2(\Delta\Phi_2) P_{\Delta\bar{\vartheta}} E \quad (106)$$

where  $\Delta\Phi_j$  are the changes (due to fluctuations) in  $\Phi_j$  between the two successive applications of the pushing gate, that is

$$\Delta\Phi_j = (\Phi_j)_{G_2} - (\Phi_j)_{G_1}, \quad (107)$$

while  $\Delta\bar{\vartheta}$  is the change in  $\bar{\vartheta}$ , that is

$$\Delta\bar{\vartheta} = \bar{\vartheta}_{G_2} - \bar{\vartheta}_{G_1}. \quad (108)$$

Notice that for  $\Delta\Phi_j = 0$  and  $\Delta\bar{\vartheta} = 0$  (no fluctuations), the sequence (105) corresponds to the sequence (29) and both error operators  $E_1$  and  $E_2$  are equal to  $E$  in Eq. (15).

The imprecision represented by  $\Delta\bar{\vartheta}$  is similar in its effects to those of  $\delta\vartheta$  because it reduces the fidelity by an amount of the order of  $(\Delta\bar{\vartheta})^2$  in the limit  $\Delta\bar{\vartheta} \ll 1$ .

The imprecision represented by  $\Delta\Phi_j$  can be regarded as an imprecision of the second  $\pi$  pulse and hence is an example of the case which was treated in Sec. II F, namely a unitary error in a  $\pi$  pulse having the form of a rotation about the  $z$  axis of the Bloch sphere. The effect on the fidelity is given by Eq. (42) with  $\varepsilon_j = \Delta\Phi_j$  and  $p_j = 0$ . For example, in the case where  $\Delta\Phi_j$  is caused by laser intensity noise, the contribution to the infidelity is of order  $[C(\Delta I/I)]^2$ , where  $\Delta I$  is the fluctuation in laser intensity between the two applications of the gate operation  $G$ , and the constant  $C$  is of order  $d/\xi a \simeq 500$ . Thus, fluctuations of order  $\Delta I/I \sim 10^{-3}$  would be sufficient to render the gate useless.

### B. Cancellation of single-qubit phase fluctuations

We now propose a method to greatly reduce the sensitivity to fluctuations. We will assume that the fluctuations  $\Delta\Phi_j$  are caused by fluctuations in the pushing force, and we assume that the force may vary, but  $s$  does not. This case holds whenever the force comes from a gradient of some potential, and the size but not the shape of that potential can fluctuate. The analysis therefore applies to the case of an optical dipole force with laser intensity noise. An analysis with appropriate modifications would apply if the source of fluctuations was another parameter such as the trapping frequency  $\omega$  hidden in the parameter  $a$  or the trap distance  $d$ .

The essence of the idea is to work at a stationary value of single-qubit phase, i.e.  $d\Phi_j/d\xi = 0$ . This can be done by choosing parameters such that the contribution from the light shift just cancels the contribution from the Coulomb energy. The Coulomb contribution (the fourth term in Eq. (103)) is proportional to the size of the force ( $\xi \sim F$ ), while the light shift contribution (the third term in Eq. (103)) is proportional to the size of light shift itself ( $s\xi \sim E$ ). Therefore, we have to balance the gradient of the light shift with its size. This can be done by choosing a convenient distance scale  $s$  for the laser beams.

To calculate the optimal value for  $s$ , we now have to reconsider the analysis, taking force fluctuations into account. The effect is that the parameter  $\xi$  now depends on time, where  $\xi$  is expressed in Eq. (94) giving  $\xi \propto |\Omega_0|^2 \propto I$ . The analysis in previous sections is unchanged except that wherever previously we wrote  $\xi$ , now we must put a mean value  $\langle \xi \rangle$ , where the details of how the averaging takes place will depend on how  $\xi$  appears in the formulae, and the mean value is taken over the gate time  $\tau$ . We will not discuss such details, but simply use the formulae, replacing  $\xi^n$  by  $\langle \xi^n \rangle$ . To estimate the changes in  $\Phi_j$  due to fluctuations in  $\xi$ , let us calculate the derivative of  $\Phi_j$  giving

$$\frac{d\Phi_1}{d\xi} = \sqrt{\frac{\pi}{8}} \epsilon \omega \tau \left[ \frac{\mathcal{A}}{\epsilon} - \frac{s \sqrt{8}}{a \epsilon} - \frac{d}{a} \frac{1}{\sqrt{2}} + \mathcal{O}(a/d) \right], \quad (109)$$

where

$$\mathcal{A} = \left[ 1 - \frac{\epsilon}{2} - \frac{1}{(\omega\tau)^2} \right] \frac{d\langle \xi^2 \rangle}{d\xi}, \quad (110)$$

with a similar expression for  $d\Phi_2/d\xi$  with the replacements  $s \rightarrow s'$  and  $d \rightarrow -d$ .

The pushing force  $F$  is derived from a potential which we shall call  $V_F$ , defined in such a way that for either ion,  $x = 0$  ( $z = 0$ ) is the position occupied by the ion before the force is applied. For example, for the travelling-wave (TW) and standing-wave (SW) configuration discussed in Sec. V we may write

$$V_F = \begin{cases} V_0 e^{-2[(x-x_0)/w]^2}, & \text{(TW)} \\ V_0 \sin^2[k(z-z_0)], & \text{(SW)} \end{cases} \quad (111)$$

where  $V_0 = V_0(t)$  is a function of time. In what follows we use the position variable  $x$  but we understand that it changes to  $z$  in the case of the standing-wave. We introduced the potential energy into the Hamiltonian (56) in the form  $(s-x \pm d/2)F$ , where after the transformation (59) it is  $(s-x)F$ . Then, we have

$$(s-x)F \equiv V_F(x) = V_F(0) + x \frac{dV_F}{dx}(0) + \mathcal{O}(x^2), \quad (112)$$

hence

$$s = -\frac{V_F(0)}{V'_F(0)} = \begin{cases} -w^2/4x_0, & \text{(TW)} \\ \tan(kz_0)/2k, & \text{(SW)} \end{cases} \quad (113)$$

where  $V'_F(0) = \frac{dV_F}{dx}(0)$  for TW,  $V'_F(0) = \frac{dV_F}{dz}(0)$  for SW and we neglected terms of order  $x^2$  ( $z^2$ ) and above. The same relations apply for the parameter  $s'$  (ion 2). We see from Eq. (113) that  $s$  and  $s'$  can be tuned by adjusting the size of the beam waist  $w$  (or standing-wave period  $k$ ) or the position  $x_0$  ( $z_0$ ) or both. The reference position  $x_0$  ( $z_0$ ) and the waist  $w$  can be chosen independently for each ion if so desired. The standing-wave period  $k$  is tunable without changing the laser wavelength by adjusting the angle between the beams forming the standing wave.

There exists a ‘‘sweet spot’’ or an optimal choice for the parameters  $s$  and  $s'$  which cancels  $d\Phi_1/d\xi$  and  $d\Phi_2/d\xi$ , namely

$$s = -\frac{\epsilon d}{4} + \frac{a}{\sqrt{8}} [\mathcal{A} + \epsilon \mathcal{O}(a/d)], \quad (114a)$$

$$s' = +\frac{\epsilon d}{4} + \frac{a}{\sqrt{8}} [\mathcal{A} + \epsilon \mathcal{O}(a/d)], \quad (114b)$$

which we obtained from Eq. (109) for  $d\Phi_j/d\xi = 0$ . Typically,  $\epsilon d \gg a$  so this implies that the parameters  $s$  and  $s'$  have opposite signs. There are two possibilities. Either (i) the pushing forces act on the two ions in the same direction, but the potential energy  $V_F(0)$  has opposite sign at the two ions, or (ii) the pushing forces act in opposite directions and the potential energies have the same sign.

In the first case (forces in the same direction), Eqs. (114) are valid. However, either in the standing-wave configuration or in the travelling-wave configuration (with both laser beams derived from the same laser), the light shifts have the same sign at the two ions. Therefore, we must have the second case (forces in opposite directions) and we have to consider a situation different to the one treated up till now. We could eventually consider the first case if we applied opposite detunings for two consequent applications of the gate pulse  $G$ . This would also directly implement the effect of the  $\pi$ -pulse method without using any  $\pi$  pulses [11].

With forces in opposite directions, a phase gate is still produced with the same pulse timings, but now the single-qubit phases are changed. The simplest way to analyse this is to make the replacement  $F_\beta(t) \rightarrow -F_\beta(t)$  in Eq. (56). It means that we reverse the force on ion 2 (compared to ion 1) but we preserve the relationships given in Eq. (57) and (113). Carrying the analysis through, we find that the single-particle potential energy phase is

$$\phi'_\beta = \sqrt{\frac{\pi}{8}} \beta \omega \tau \xi^2 + \sqrt{\pi} \beta \omega \tau \xi \frac{s'}{a}, \quad (115)$$

in contrast this with Eq. (79). The two-particle phases  $\phi_{\alpha\beta}$  are as described in Appendix E with the replacement  $\beta \rightarrow -\beta$ . Hence we now have

$$\Phi_2 = \theta \left[ -\frac{1}{\epsilon(\omega\tau)^2} + \frac{1}{\epsilon} + \frac{s' \sqrt{8}}{a \xi \epsilon} - \frac{d}{a} \frac{1}{\xi \sqrt{2}} - \frac{1}{2} + \mathcal{O}(a/d) \right], \quad (116)$$

so the “sweet spot” is

$$s' = +\frac{\epsilon d}{4} - \frac{a}{\sqrt{8}}[\mathcal{A} + \epsilon \mathcal{O}(a/d)]. \quad (117)$$

Note that  $s$  and  $s'$  still have opposite signs, but now (114a) and (117) apply for the situation with light shifts at the two ions of the same sign and pushing forces on the two ions in opposite directions. Example cases will be given in Sec. VIII.

## VII. NON-UNIFORM PUSHING FORCE

The original proposal [8] assumed that the pushing force is uniform. However, we introduced the optical dipole force as a suitable candidate for the pushing force, where the dipole force originates from a non-uniform intensity profile of a laser beam. Therefore, the ions experience a pushing force which depends on their position. In their thermal vibrational motion the ions explore different positions and as a result the force they experience depends on their thermal motion. In this section we will analyse this by allowing the dimensionless amplitude of the force  $\xi$  introduced in Eq. (66) to be a spatial function rather than a constant (as we have considered up till now).

Using  $F(x, t) = -dV_F(x, t)/dx$  we obtain from Eq. (111) the amplitude of the pushing force for the travelling-wave configuration

$$\xi_{\text{trav}}(x) = \xi_0 \frac{x_0 - x}{x_0} e^{-2(x^2 - 2x_0x)/w^2}, \quad (118)$$

where  $\xi_0 = \xi_{\text{trav}}(0)$  and  $x_0$  refers to the ion position in cross-section of the laser beam profile. For the standing-wave configuration we get

$$\xi_{\text{stan}}(z) = \xi_0 \frac{\sin[2k(z_0 - z)]}{\sin(2kz_0)}, \quad (119)$$

where  $\xi_0 = \xi_{\text{stan}}(0)$  and  $z_0$  refers to the position of the ion in the standing-wave field.

The non-uniformity of the pushing force introduces an additional probabilistic character to the phase  $\Theta_{\alpha\beta}$  because the amplitude  $\xi$  appears in all expressions for single-particle and two-particle phases. Once the value of  $\xi$  is not known precisely it introduces a further imprecision to the system and, consequently, a drop of the fidelity.

The  $\pi$ -pulse method is again a useful tool because it goes some way towards alleviating the effects of the non-uniformity in the pushing force. In the full quantum approach we would model a thermal state of motion by a mixture of vibrational energy eigenstates  $|n\rangle$ , then each state  $|n\rangle$  in the mixture acquires a different single-qubit phase owing to the different average force it experiences. However, as long as the heating rate is low, then the same phase will appear in both implementations of the operation  $G$  and so it is cancelled by the  $\pi$ -pulse method.

Hence, recalling Eq. (36), (37) and (81), we find that the fidelity of the phase gate with  $\pi$  pulses will depend only on two-particle phases. To calculate the fidelity we need to estimate the difference  $\delta\vartheta = \vartheta - \bar{\vartheta}$  between the actual and estimated value of the overall phase of the gate. In view of the vibrational motion of the ion in the non-uniform laser beam profile, a good estimate for the phases (compared to Eq. (84)) is now the average value

$$\bar{\vartheta} = \int_0^{2\pi} \frac{d\psi_1 d\psi_2}{(2\pi)^2} \int_0^{+\infty} \frac{d\mathcal{E}_1 d\mathcal{E}_2}{(k_B T)^2} e^{-(\mathcal{E}_1 + \mathcal{E}_2)/k_B T} \int_{-\infty}^{+\infty} dx \vartheta P(x), \quad (120)$$

where we model the ion’s position by a Gaussian probability distribution

$$P(x) = \frac{1}{\sigma\sqrt{2\pi}} e^{-x^2/2\sigma^2}. \quad (121)$$

The calculation method we have adopted here is slightly different from the approach in Section IV. We have not analysed the ion trajectories in detail. Owing to the dependence of the force on position they are now further complicated. However, in the limit where the relative change in force with position is small, the ion samples a small range of force values during its motion. In the adiabatic limit where many vibrational oscillations occur during the gate time, we assume the main effect is that the size of the force must be replaced by an average value, but otherwise the previous calculation of the dynamical phases still applies.

Eq.(121) is the positional distribution for a classical particle confined in a harmonic potential at the temperature  $T$  where the standard deviation  $\sigma$  is given by

$$\frac{1}{2}m\omega^2\sigma^2 = \frac{1}{2}k_B T. \quad (122)$$

It is useful to express this in terms of the quantum harmonic oscillator energy levels, giving

$$\sigma = \sqrt{\frac{k_B T}{m\omega^2}} \approx a\sqrt{\langle n \rangle}, \quad (123)$$

where  $\langle n \rangle \approx k_B T/\hbar\omega$  is the mean vibrational number and  $a = \sqrt{\hbar/m\omega}$ .

Now we have all the tools to calculate the fidelity of the phase gate with  $\pi$  pulses for the non-uniform pushing force. The fidelity depends on the departures  $\delta\vartheta$  of the phase from its average (estimated) value, in other words on the variance of the distribution of  $\vartheta$  values. This is calculated in Appendix F, where a complete expression, evaluated up to order  $(a/d)^4$  and to  $(a/w)^4$  for the travelling wave, and to all orders in  $a/\lambda$  for the standing-wave case, is set out. The most important terms in

the travelling-wave case are given by

$$\begin{aligned} \mathcal{F}' &\simeq 1 - \left( \frac{6\theta_0 k_B T}{\hbar\omega} \right)^2 \left( \frac{a}{d} \right)^4 \\ &\quad - \frac{2\theta_0}{3} \left( \frac{6\theta_0 k_B T}{\hbar\omega} \right) \left( \frac{a}{w} \right)^2 \left( \frac{2x_0}{w} - \frac{w}{2x_0} \right)^2 \\ &\quad - \frac{2}{9} \left( \frac{6\theta_0 k_B T}{\hbar\omega} \right)^2 \left( \frac{a}{w} \right)^4 \mathcal{Q}(2x_0/w), \end{aligned} \quad (124)$$

where  $\mathcal{Q}(y) = 12y^4 - 64y^2 + 89 - 34/y^2 + 1/y^4$  and  $2\theta_0 \approx \pi$ . This expression has been written as a power series in  $a/w$  and it is sufficiently accurate to give the behaviour for all the cases considered in Sec. VIII. The first term corresponds to the fidelity with the uniform force in Eq. (88). However, in practice the other terms almost always dominate because  $w < d$ . The second term vanishes when  $x_0 = w/2$ , but away from this position it dominates. Therefore, placing the ion at  $w_0 = w/2$  offers a useful improvement in fidelity.

In the standing-wave case, the expression for the fidelity simplifies considerably when the ion position is chosen as  $kz_0 = \pi/4$ . This is also the best choice to maximize the fidelity. Restricting to this choice for the ion position, the most important terms in the standing-wave case are

$$\mathcal{F}' \simeq 1 - \frac{\theta_0^2}{32} \left\{ 1 - \exp \left[ -16(ka)^2 \left( \frac{k_B T}{\hbar\omega} \right) \right] \right\}^2. \quad (125)$$

This reproduces the full expression to good accuracy except when  $\mathcal{F}' \lesssim 0.9$ .

## VIII. TOTAL INFIDELITY

We will now bring together all the contributions to infidelity which have been discussed, in order to examine the performance of the gate in practice. These contributions are: (i) inaccuracy between actual  $\Theta_{\alpha\beta}$  and estimated phases  $\bar{\Theta}_{\alpha\beta}$ , (ii) imprecision of the  $\pi$  pulses, (iii) photon scattering, (iv) laser intensity fluctuations and (v) non-uniform character of the pushing force. We will use parameters for the calcium ion to give examples.

Ignoring photon scattering for a moment, it follows from Eq. (51) that the fidelity of the phase gate is

$$\tilde{\mathcal{F}} = (1 - 4\zeta)(1 - \mathcal{P}'), \quad (126)$$

where we introduced *infidelity*  $\mathcal{P}' \equiv 1 - \mathcal{F}'$  and  $\mathcal{F}'$  is given by Eq. (124) or (125), respectively. The effect of laser intensity fluctuations can be absorbed into the term  $\zeta$  representing imperfection of the  $\pi$  pulses (see the discussion in the last paragraph in Sec. VIA).

The influence of photon scattering further reduces the fidelity. We have not calculated in detail the combination of all effects at once, but the expected behaviour is that the fidelities multiply, or the infidelities add. In

the limit of small infidelity these two statements agree. Therefore, using Eq. (102) and (126), we estimate the total infidelity, including all effects, to be  $\mathcal{F}_{\text{tot}} = \mathcal{F}'\mathcal{F}_{\text{scat}}$ , giving

$$\mathcal{P}_{\text{tot}} \simeq 4\zeta + \mathcal{P}' + N, \quad (127)$$

where we assumed all the contributions are small compared to one ( $\zeta, \mathcal{P}', N \ll 1$ ) and  $2\theta_0 \approx \pi$ .

### A. Analysis

We would like to minimize the infidelity while maximizing desirable features such as gate speed. The overall problem has 11 parameters. Two are associated with the design of the ion traps:

- $\omega$  – trapping frequency,
- $d$  – trap separation.

Four are associated with the laser beam:

- $P$  – laser power,
- $w$  ( $\pi/k$ ) – size of the waist of the beam (period of the standing wave),
- $\Delta$  – detuning of the laser,
- $x_0$  ( $z_0$ ) – position of the ion in the profile of the beam (in the standing-wave field).

Two describe unavoidable imperfections:

- $T$  – temperature,
- $\zeta$  – imperfection of the  $\pi$  pulses.

Finally, the last three parameters are associated with the ion and the transition which provides the light shift:

- $m$  – mass of the ion,
- $\lambda_{\text{atom}}$  – wavelength of a dipole transition,
- $\Gamma$  – linewidth of that transition.

We will assume the last three parameters are “given”, i.e. they cannot be varied in seeking the best behaviour. We will also assume that  $\zeta$  is negligible ( $\zeta \ll \mathcal{P}_{\text{tot}}$ ). This implies that the  $\pi$  pulses are assumed to be precise, and that the laser intensity noise is small. We find that in all cases to be considered, the force is only sufficient to displace the ions by a small fraction of the trap distance ( $\bar{x}/d \sim 10^{-2} - 10^{-3}$ ), and therefore the “sweet spot” may be needed to suppress the effect of intensity noise sufficiently for this assumption to be valid.

The position of the ion in the laser beam should be chosen sensibly. For the travelling wave, the temperature effects (124) are minimized at  $x_0 = w/2$  (the position of maximum force), but photon scattering (97) is minimized at  $x_0 = w/\sqrt{2}$ . Since the fidelity  $\mathcal{F}'$  depends more sharply on  $x_0$  than the number of scattered photons, we will adopt the former choice, i.e.  $x_0 = w/2$ . For



the standing wave we chose  $kz_0 = \pi/4$  (and  $x_0 = 0$ ) for the same reason.

The remaining parameters are  $\omega$ ,  $d$ ,  $P$ ,  $w$ ,  $k$ ,  $\Delta$  and  $T$ . We will examine a range of values of  $\omega$  and  $d$ , subject to technological constraints on what is feasible for the trap construction. For the temperature, we keep in mind that ion traps in general have three temperature regimes which may be relevant: (i) the Doppler limit temperature  $k_B T = \hbar\Gamma/2$ , (ii) cooling to near the ground state  $\langle n \rangle \approx k_B T / \hbar\omega \simeq 1$ , and (iii) ground state cooling  $\langle n \rangle \ll 1$ . The regime (i) is achieved by standard Doppler cooling techniques, the regime (iii) by the more technically demanding sideband cooling, and the intermediate case is attractive because it can be achieved by Doppler-type cooling on a narrow transition (i.e. using a two-photon resonance). Since the gate under consideration is relatively insensitive to temperature effects, we will avoid assuming ground state cooling, by choosing either the Doppler limit temperature or  $\langle n \rangle \simeq 1$ .

Now it only remains to specify the laser parameters  $P$ ,  $w$ ,  $k$  and  $\Delta$ . In most conditions higher laser power  $P$  acts in a beneficial way, so the correct choice is the highest power available (exceptions to this rule can occur when the laser detuning  $\Delta$  becomes of the order of internal transition frequencies in the ion). The spot size  $w$  (for the travelling wave) or the period  $\pi/k$  (for the standing wave) has to make a compromise. A smaller value increases the force, which reduces the photon scattering, but the smaller value also increases the sensitivity to temperature through Eq. (124) and (125).

It is noteworthy that the total fidelity does not depend on the laser detuning  $\Delta$  (in the weak-coupling regime, i.e.  $|\Omega| \ll |\Delta|$ ). The detuning  $\Delta$  can be adjusted to set the size of the force ( $\xi \propto 1/\Delta$ ) and hence the speed of the gate ( $\tau \propto 1/\xi^2$ ).

FIG. 6 and FIG. 7 show the total infidelity as a function of trapping frequency, for various values of trap separation. The laser parameters are set equal to the technically undemanding values  $P = 10$  mW and  $w = 4$   $\mu\text{m}$ . Results for two cooling regimes are shown: either the Doppler limit for calcium on a dipole-allowed transition, or cooling to  $\langle n \rangle \simeq 1$ . FIG. 8 and FIG. 9 show results for the more demanding laser parameters  $P = 100$  mW and  $w = 2$   $\mu\text{m}$ . We see immediately that good fidelity can be attained, even at the Doppler limit temperature.

Next, let us examine  $\bar{x}/d \sim a\xi/d$  in order to learn the size of the single-qubit phases. Using Eq. (70) and (82) we find

$$\frac{a\xi}{d} \approx \sqrt{\frac{\omega d}{v}}, \quad (128)$$

where we introduced the characteristic velocity  $v = \omega\tau\ell\sqrt{8}/(\hbar\sqrt{\pi}) \approx 1.6(\omega\tau)\alpha c$ ,  $\alpha$  is the fine structure constant,  $c$  is the speed of light,  $\ell$  was defined in Eq. (56) and  $2\theta \approx \pi$ . We would like  $\bar{x}/d$  to be small but not too small. We therefore choose the gate time  $\tau$  to be small, which also gives the fastest possible gate. The limit is set

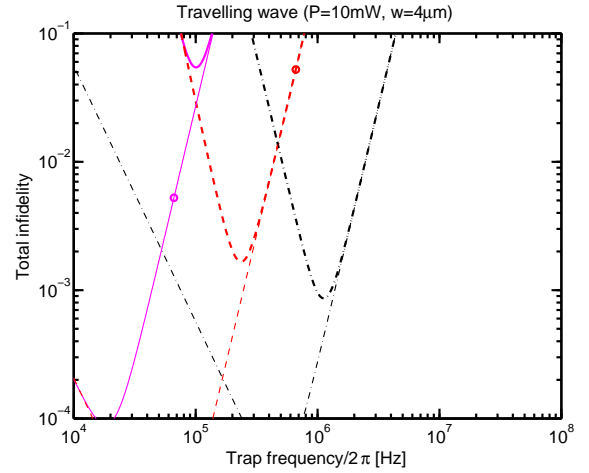


FIG. 6: The total infidelity given by Eq. (127) as a function of the trap frequency for various parameter values for the travelling-wave configuration. Results shown are for laser parameters  $P = 10$  mW and  $w = 4$   $\mu\text{m}$ . The solid lines are for the trap separation  $d = 100$   $\mu\text{m}$ , the dashed lines are for  $d = 10$   $\mu\text{m}$  and the dash-dotted lines are for  $d = 1$   $\mu\text{m}$ . The thick lines are for the temperature equal to the Doppler limit temperature associated with the dipole-allowed  $4S_{1/2} \leftrightarrow 4P_{1/2}$  transition at  $\lambda = 397$  nm in  $\text{Ca}^+$ , i.e.  $T = 538$   $\mu\text{K}$ . The thin lines are for  $k_B T = \hbar\omega$ , i.e.  $\langle n \rangle \simeq 1$ . The circles show the “sweet spot” condition (129).

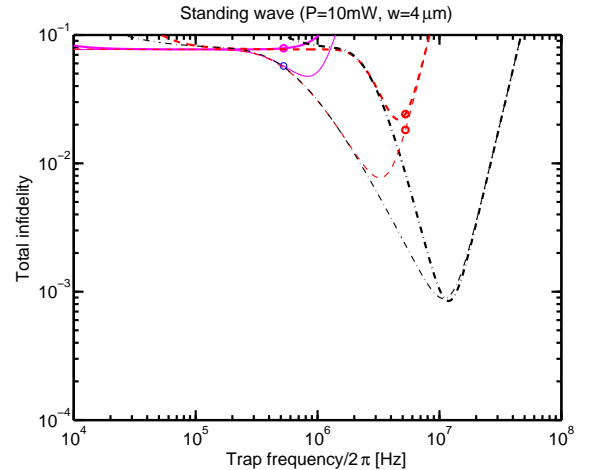


FIG. 7: Same as FIG. 6, but for the standing-wave configuration.

by the adiabatic condition  $\omega\tau \gg 1$ . The non-adiabatic terms fall off exponentially with  $(\omega\tau)^2$  so a modest value  $\omega\tau = 5$  is sufficiently large, hence  $v = 1.8 \times 10^7$   $\text{m} \cdot \text{s}^{-1}$ . FIG. 6–9 show that the value of  $\omega d$  must be of order  $10^2 - 10^3$   $\text{m} \cdot \text{s}^{-1}$  in order to obtain high fidelity, therefore we find  $a\xi/d$  is in the range  $2 \times 10^{-3} - 8 \times 10^{-3}$ . This implies that in order to keep the single-qubit phase fluctuations sufficiently small it may be necessary to impose the “sweet spot” condition. For a given laser beam size and given trap separation, this is a condition on the trap-

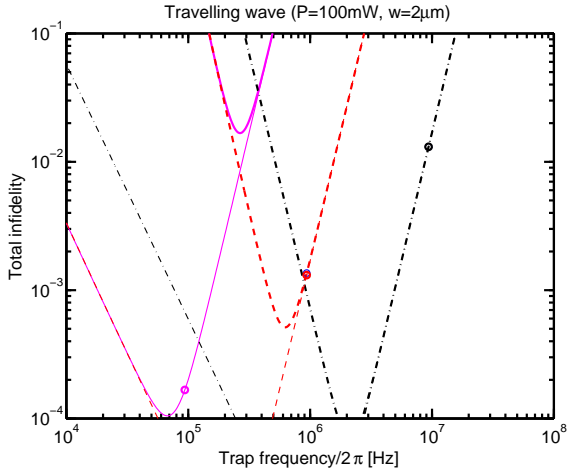


FIG. 8: Same as FIG. 6, except now the laser parameters are  $P = 100$  mW and  $w = 2 \mu\text{m}$ .

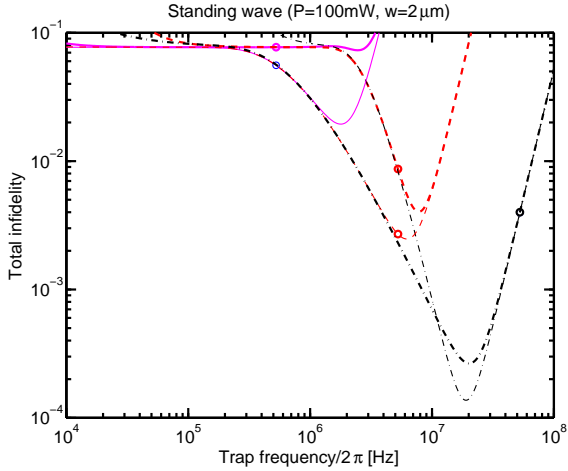


FIG. 9: Same as FIG. 8, but for the standing-wave configuration.

ping frequency

$$\omega_{\text{sweet}} \approx \frac{1}{d} \sqrt{\frac{\ell}{m|s|}}, \quad (129)$$

where we approximated Eq. (114) to the form  $|s| \approx \epsilon d/4$ , since we find the parameter values are such that the second term in Eq. (114) is a small adjustment. The “sweet spot” values of  $\omega$  are indicated by the circles in FIG. 6–9. If the “sweet spot” requirement is imposed, one can no longer tune  $\omega$  so as to minimize the infidelity.

A further constraint (in addition to the adiabatic approximation), which affects the gate rate, is the condition that the ion is not pushed too far (we will assume  $\bar{x} \lesssim w/4$  for the travelling wave and  $\bar{x} \lesssim \lambda/10$  for the standing wave). Otherwise the ion will move into a region where the light shift gradient is substantially reduced, the net result would be a slower gate and increased

photon scattering. Using Eq. (128) we can write

$$\omega\tau \approx \left( \frac{d}{\bar{x}_{\text{max}}} \right)^2 \frac{\omega d}{\alpha c}, \quad (130)$$

where  $\bar{x}_{\text{max}} = a\xi$  now denotes the maximum distance the ion is allowed to move. We choose  $\bar{x}_{\text{max}} = w/4$  ( $\bar{x}_{\text{max}} = \lambda/10$ ) for the travelling (standing) wave. Taking the “sweet spot” value for  $\omega d$  from Eq. (129), we find that Eq. (130) gives the limiting condition on  $\omega\tau$  (i.e.  $\omega\tau \gtrsim 5$ ) for the standing-wave case when  $d \gtrsim 7 \mu\text{m}$  and for the travelling-wave case when  $d \gtrsim 220 \mu\text{m}$  at  $w = 2 \mu\text{m}$ . In general one might expect the larger light shift gradient to allow the gate to be faster for the standing wave compared to the travelling wave. Owing to the previous findings, however this is no longer true when the trap separation  $d$  is large, i.e. of the order of  $50 \mu\text{m}$  or above.

We find the laser detuning  $\Delta$  becomes comparable to the fine structure splitting ( $4P_{1/2} \leftrightarrow 4P_{3/2}$ ) of  $\text{Ca}^+$  in the case of the travelling wave for  $P = 100$  mW and  $w = 2 \mu\text{m}$ , but in the other cases the detuning is not too large. This would reduce the ratio of pushing force size to photon scattering rate, if the qubit is stored in the ground state manifold, and therefore result in more photon scattering.

We also find that  $\epsilon \ll 1$  for the cases in FIG. 6–9, where the fidelity is high.

## B. Discussion

Although our study has shown that the pushing gate in practice does not offer as high a fidelity as was predicted in the initial papers which described it, nevertheless comparing this gate with others (which have been proposed for ion trap quantum computers), it retains a very good combination of allowed temperature and gate rate. The 1995 proposal of Cirac and Zoller [1] required ground state cooling  $\langle n \rangle \ll 1$  and required the gate rate  $R$  to be small compared to  $\eta\omega$ , where  $\eta$  is the Lamb-Dicke parameter [12]. The work of Mølmer and Sørensen [13–15] and others has revealed methods which allow the requirement on cooling to be relaxed to  $\langle n \rangle \ll 1/\eta^2$ . The “pushing gate”, by contrast, allows a fast gate rate  $R = 1/2\tau \simeq \omega/10$ , with simultaneously high temperature. The standing-wave configuration places the stronger constraint on temperature, but even for this case the Lamb-Dicke condition  $\langle n \rangle \ll 1/\eta^2$  is sufficient.

The examples with  $P = 10$  mW and  $w = 4 \mu\text{m}$  show that the gate could be demonstrated with modest requirements on the laser beam power and size. A trap separation below approximately  $100 \mu\text{m}$  would be needed which is of the order of the smallest values which have been reported for ion trap experiments up till now.

It is reasonable to expect that  $d = 10 \mu\text{m}$  may become available in the (near) future. This would permit the infidelity to fall to  $\mathcal{P}_{\text{tot}} \sim 1 \times 10^{-3}$  at the Doppler limit

temperature, by using the travelling-wave configuration at  $P = 100$  mW,  $w = 2$   $\mu$ m and  $\omega/2\pi = 1$  MHz, giving a gate time of  $10/\omega = 1.6$   $\mu$ s. The same laser parameters with the standing-wave configuration would allow a gate time of  $0.3$   $\mu$ s at infidelity  $\mathcal{P}_{\text{tot}} \sim 7 \times 10^{-3}$ .

In the longer term it would be desirable to have a system consisting of a large number ( $> 10^3$ ) of trap pairs, with many gate operations performed simultaneously. With trap separations of the order of micrometres and a gate rate of order 10 MHz, the infidelity of order  $4 \times 10^{-4}$  would be available if the laser intensity noise were small enough. However reducing the total laser power may become an important consideration for a large processor.

## IX. CONCLUSION

The main results of this paper are:

(i) The single-qubit rotations have contributions from the Coulomb repulsion, the light (AC Stark) shift, the trapping potential, and the kinetic energy. When the parameter regime is such that the two-qubit phase is insensitive to ion temperature, then the Coulomb contribution to the single-qubit phases is much larger than  $\pi$  ( $\sim 500\pi$ ) and proportional to the size of the pushing force. This is dangerous because it implies that laser intensity fluctuations just of the order of  $10^{-3}$  could be sufficient to destroy the fidelity.

(ii) The dipole force was introduced. It is found that the number  $N$  of scattered photons during the gate varies as  $\lambda/P$  for wavelength  $\lambda$  and laser power  $P$  for a laser beam focused such that the waist size is proportional to the wavelength. Surprisingly, photon scattering is independent of the detuning  $\Delta$  and the atomic transition linewidth  $\Gamma$  in the limit  $|\Omega|, \Gamma \ll |\Delta|$ , where  $\Omega$  is the Rabi frequency. The infidelity associated with photon scattering increases with the trap separation  $d$  and the trapping frequency  $\omega$ , while the infidelity associated with finite ion temperature falls with  $d$  and  $\omega$ . The best compromise is such that if the separation is small, the frequency should be large. It is found that very good fidelity can be obtained for reasonable values of the parameters (see FIG. 6–9).

(iii) A lack of spatial uniformity in the pushing force is found to be a significant consideration when the distance scale ( $w$  or  $\pi/k$ ) of the force profile is smaller than the separation  $d$  of the ions. In this situation, the effect of a finite temperature of the ions is primarily to cause fluctuations in the size of the force they experience, and hence fluctuations in the phase of the gate. Nevertheless, the gate performs well for reasonable values of the parameters, and cooling to the motional ground state is not needed.

(iv) Using the  $\pi$ -pulse method (“spin-echo”), we find that a given infidelity ( $\zeta$  or  $\varepsilon^2$ ) in the  $\pi$  pulses simply reduces the overall fidelity by approximately  $\zeta$  or  $\varepsilon^2$ . An equivalent error occurs if a parameter of the push-

ing gate changes slightly between two successive applications. The most likely source of such fluctuations is laser intensity noise. It is shown that the single-qubit phases can be made first order insensitive to laser intensity noise, by choosing the distance scale (“sweet spot”) of the laser intensity gradient so that the AC Stark light shift balances the contribution from Coulomb repulsion. This greatly reduces the requirement on laser intensity stability, indeed in practical terms it may make the difference between a feasible gate and an unfeasible one.

To conclude overall, the analysis of the points summarized above was necessary to assess the “pushing gate”, and to gain insight into its physical mechanism. The analysis which has been presented is sufficiently complete to describe an experimental realisation. Even though it was found that the fidelity of the gate will not be as high as was originally predicted, it still performs well in that (i) it does not require ground state cooling and (ii) with sufficient laser power neither is cooling to the Lamb-Dicke limit required, while the gate time can be close to the inverse of trap vibrational frequency, making it a fast gate in comparison with others which have been proposed for ion traps.

## Acknowledgments

We wish to acknowledge helpful conversations with T. Calarco and the opportunity to see some numerical results by V. Barone and S. Garelli. This work was supported by the EPSRC and the Research Training, Development and Human Potential Programs of the European Union (QUEST and QUBITS).

## APPENDIX A: FIDELITY OF DIAGONAL UNITARY MATRICES

Suppose a physical operation designed to produce some logical operation  $U$  instead produces  $G$ , where  $G \neq U$ . The fidelity is then defined to be

$$\mathcal{F} = \min_{|\Psi_0\rangle} |\langle \Psi_0 | U^\dagger G | \Psi_0 \rangle|^2, \quad (\text{A1})$$

where

$$|\Psi_0\rangle = \sum_{\alpha, \beta=0}^1 c_{\alpha\beta} |\alpha\beta\rangle \quad (\text{A2})$$

is an arbitrary two-qubit state denoting  $|\alpha\beta\rangle = |\alpha\rangle \otimes |\beta\rangle$ .

Next we will calculate  $\mathcal{F}$  for some cases of interest when the operator  $U^\dagger G$  is diagonal and unitary. Therefore, let us consider a general diagonal operator of two qubits

$$U^\dagger G = \text{diag}\{e^{i\Theta_{00}}, e^{i\Theta_{01}}, e^{i\Theta_{10}}, e^{i\Theta_{11}}\}. \quad (\text{A3})$$

Without a loss of generality we may extract  $\Theta_{00}$  as a global phase and relabel Eq. (A3) as follows

$$U^\dagger G = \text{diag}\{1, e^{i\theta_{01}}, e^{i\theta_{10}}, e^{i\theta_{11}}\}. \quad (\text{A4})$$

When we now substitute Eq. (A4) to (A1) we get

$$\mathcal{F} = \min_{w,x,y,z} (1 - 4f) \quad (\text{A5})$$

with

$$\begin{aligned} f = & wx \sin^2(\theta_{01}/2) + wy \sin^2(\theta_{10}/2) + wz \sin^2(\theta_{11}/2) \\ & + xy \sin^2[(\theta_{01} - \theta_{10})/2] + xz \sin^2[(\theta_{01} - \theta_{11})/2] \\ & + yz \sin^2[(\theta_{10} - \theta_{11})/2], \end{aligned} \quad (\text{A6})$$

where to make the expressions less cluttered we used the notation

$$\{w, x, y, z\} \equiv \{|c_{00}|^2, |c_{01}|^2, |c_{10}|^2, |c_{11}|^2\}. \quad (\text{A7})$$

The normalisation  $w + x + y + z = 1$  may be used to reduce  $f$  to a function of three variables  $f = f(x, y, z)$  with three parameters  $\theta_{01}, \theta_{10}, \theta_{11}$ .

To find the minimum fidelity  $\mathcal{F}$ , the function  $f$  must be maximised. The general case is straightforward to calculate but leads to a complicated expression without much useful insight. It is more valuable to consider some special cases.

(i) When one phase is negligible compared to the others (for instance  $\theta_{11} \ll \theta_{01}, \theta_{10}$ ), using the normalisation condition we have

$$\begin{aligned} f(x, y) \approx & (1 - x - y)[x \sin^2(\theta_{01}/2) + y \sin^2(\theta_{10}/2)] \\ & + xy \sin^2[(\theta_{01} - \theta_{10})/2]. \end{aligned} \quad (\text{A8})$$

Since this is now a function of only two variables  $x$  and  $y$  the maximisation is easier to calculate but still does not yield a concise answer.

(ii) For the case  $\theta \equiv \theta_{10} = \theta_{01} \gg \theta_{11}$ , from Eq. (A8) we have

$$f(x, y) = (1 - x - y)(x + y) \sin^2(\theta/2), \quad (\text{A9})$$

whose maximum value is  $f_{\max} = (1/4) \sin^2(\theta/2)$  when  $x + y = 1/2$ . Hence the fidelity is

$$\mathcal{F} = 1 - \sin^2(\theta/2) = \cos^2(\theta/2). \quad (\text{A10})$$

(iii) For the case  $\theta \equiv \theta_{10} = -\theta_{01} \gg \theta_{11}$ , from Eq. (A8) we have

$$f(x, y) = (1 - x - y)(x + y) \sin^2(\theta/2) + xy \sin^2 \theta. \quad (\text{A11})$$

The maximum value is on the line  $x = y$ , where after some algebra we get from the previous expression

$$f(x) = 2x \sin^2(\theta/2)[1 - 2x \sin^2(\theta/2)]. \quad (\text{A12})$$

This function has a maximum value  $f_{\max} = 1/4$  when  $\theta \geq \pi/2$ , yielding zero fidelity ( $\mathcal{F} = 0$ ). For  $\theta \leq \pi/2$  the maximum of the function  $f$  is when  $x$  takes its largest value subject to the normalisation constraint  $2x \leq 1$ , giving  $f_{\max} = (1/4) \sin^2 \theta$ . Hence the fidelity is

$$\mathcal{F} = \cos^2 \theta \quad (\text{A13})$$

(iv) Finally, if all phases apart from one are negligible (for instance  $\theta \equiv \theta_{01} \gg \theta_{10}, \theta_{11}$ ), we have

$$f(x) = x(1 - x) \sin^2(\theta/2), \quad (\text{A14})$$

giving the fidelity  $\mathcal{F} = \cos^2(\theta/2)$ .

## APPENDIX B: ANALYSIS OF PURE “OVER-ROTATION” ERRORS OF $\pi$ PULSES

To study the effect of “over-rotation” in the  $\pi$  pulses, we assume that a single-qubit gate intended to be a  $\pi$  pulse on ion  $j$  in fact produces the effect  $R_j M_j(\varepsilon_j)$ , where  $M$  is given in Eq. (41). Therefore, the complete gate sequence replaces the one in Eq. (24), giving  $S'(RM_B)G(RM_A)G$ , where

$$M_A = M_1(\varepsilon_1) \otimes M_2(\varepsilon_2), \quad (\text{B1a})$$

$$M_B = M_1(p\varepsilon_1) \otimes M_2(p\varepsilon_2). \quad (\text{B1b})$$

Recalling Eq. (34), we find the fidelity is  $\min |\langle \Psi_0 | Q | \Psi_0 \rangle|^2$ , where

$$\begin{aligned} Q &= \left[ (G_{\text{perf}}^\dagger R^\dagger)^2 (S')^\dagger \right] [S'(RM_B)G(RM_A)G] \\ &= (G_{\text{perf}}^\dagger R^\dagger) G_{\text{perf}}^\dagger M_B G(RM_A) G. \end{aligned} \quad (\text{B2})$$

This operator, and the fidelity associated with it, does not readily simplify. We studied it by a combination of numerical searches for least fidelity, and by algebraic treatment of some less general cases. It was found that the case where both ions have the same “over-rotation” ( $\varepsilon_1 = \varepsilon_2$ ) does not lead to significantly different results from the case where the ions have different “over-rotation”. In this slightly restricted case, and considering for simplicity a perfect phase gate ( $G = G_{\text{perf}}$ ), we obtain

$$\begin{aligned} Q \approx & \mathbf{1} + \frac{i\varepsilon}{2} \begin{bmatrix} 0 & p+i & p+i & 0 \\ p-i & 0 & 0 & -(1+p) \\ p-i & 0 & 0 & -(1+p) \\ 0 & -(1+p) & -(1+p) & 0 \end{bmatrix} \\ & - \frac{\varepsilon^2}{4} \begin{bmatrix} 1+p^2-2ip & 0 & 0 & -(2p+p^2+i) \\ 0 & \chi & \chi & 0 \\ 0 & \chi & \chi & 0 \\ -p^2+i(1+2p) & 0 & 0 & (1+p)^2 \end{bmatrix}, \end{aligned}$$

where  $\chi = 1 + p^2 + (1+i)p$ . The fidelity obtained from this is of the form  $(a + bp + cp^2)\varepsilon^2$ , where the coefficients  $a, b, c$  depend on the initial state  $|\Psi_0\rangle$  under consideration. The main properties of this result are that the fidelity is found to be proportional to  $\varepsilon^2$  (not  $\varepsilon$ ) and there is no special case when  $p = 1$  or  $p = -1$ . That means the effects of two “over-rotations” by the same or by opposite amounts do not cancel.

### APPENDIX C: FIDELITY OF THE PHASE GATE WITH IMPERFECT $\pi$ PULSES

The single-qubit rotations acting on both qubits expressed by Eq. (3)–(4) can be written (up to global phases) as

$$\begin{aligned} S &= \sum_{\alpha,\beta=0}^1 |\alpha\beta\rangle\langle\alpha\beta| e^{-i\bar{\Theta}_{\alpha\beta}} (e^{i\bar{\nu}})^{\alpha\beta} \\ &= |00\rangle\langle 00| e^{-i\bar{\Theta}_{00}} + |01\rangle\langle 01| e^{-i\bar{\Theta}_{01}} \\ &\quad + |10\rangle\langle 10| e^{-i\bar{\Theta}_{10}} + |11\rangle\langle 11| e^{-i\bar{\Theta}_{11}} e^{i\bar{\nu}}. \end{aligned} \quad (\text{C1})$$

Similarly, we can rewrite the rotations  $\tilde{S}$  in Eq. (48)–(49) to the form

$$\begin{aligned} \tilde{S} &= \sum_{\alpha,\beta=0}^1 |\alpha\beta\rangle\langle\alpha\beta| e^{-i\bar{\Theta}_{\alpha\beta}} (e^{i\bar{\nu}})^{\delta_{\alpha\beta}-\alpha\beta} \\ &= |00\rangle\langle 00| e^{-i\bar{\Theta}_{00}} e^{i\bar{\nu}} + |01\rangle\langle 01| e^{-i\bar{\Theta}_{01}} \\ &\quad + |10\rangle\langle 10| e^{-i\bar{\Theta}_{10}} + |11\rangle\langle 11| e^{-i\bar{\Theta}_{11}}, \end{aligned} \quad (\text{C2})$$

where  $\delta_{\alpha\beta}$  is the Kronecker delta symbol. The two different single-qubit operations  $S$  and  $\tilde{S}$  are used here, rather than a single operation at the end, because it may be advantageous to run an experiment this way, since then imperfections in  $G$  can be undone immediately, using a feed-forward technique on the hardware which implements the gates.

Even though we introduced different bit-flip error probabilities  $\zeta_1$  and  $\zeta_2$  for the qubit 1 and 2 in Eq. (45), they will be similar in practice ( $\zeta_1 \simeq \zeta_2$ ). Here we will assume  $\zeta_1 = \zeta_2 = \zeta$ , where the error is very small ( $\zeta \ll 1$ ). We note that the overall fidelity of the whole sequence is similar in the cases  $\zeta_1 = \zeta_2$  and  $\zeta_1 \simeq \zeta_2$ .

Following the complete gate sequence (47) we can now calculate the actual state of the system (representing the evolution of the phase gate with imperfect  $\pi$  pulses) using Eq. (C1) and (C2), that is

$$\begin{aligned} \rho_{\text{act}} &\simeq (1 - 4\zeta) |\Xi_0\rangle\langle\Xi_0| \\ &\quad + \zeta \sum_{j=1}^4 |\Xi_j\rangle\langle\Xi_j| + \mathcal{O}(\zeta^2), \end{aligned} \quad (\text{C3})$$

where

$$\begin{aligned} |\Xi_0\rangle &= \sum_{\alpha,\beta} c_{\alpha\beta} e^{i(\Theta_{\alpha\beta} + \Theta_{\alpha'\beta'})} (e^{i\bar{\nu}})^{\alpha\beta + \delta_{\alpha'\beta'} - \alpha'\beta'} |\alpha\beta\rangle, \\ |\Xi_1\rangle &= \sum_{\alpha,\beta} c_{\alpha\beta} e^{i(\Theta_{\alpha\beta} + \Theta_{\alpha'\beta'})} (e^{i\bar{\nu}})^{\alpha\beta + \delta_{\alpha'\beta'} - \alpha'\beta'} |\alpha\beta'\rangle, \\ |\Xi_2\rangle &= \sum_{\alpha,\beta} c_{\alpha\beta} e^{i(\Theta_{\alpha\beta} + \Theta_{\alpha'\beta'})} (e^{i\bar{\nu}})^{\alpha\beta + \delta_{\alpha'\beta'} - \alpha'\beta'} |\alpha'\beta\rangle, \\ |\Xi_3\rangle &= \sum_{\alpha,\beta} c_{\alpha\beta} e^{i(\Theta_{\alpha\beta} + \Theta_{\alpha'\beta'})} (e^{i\bar{\nu}})^{\alpha\beta + \delta_{\alpha'\beta'} - \alpha'\beta'} |\alpha'\beta'\rangle, \\ |\Xi_4\rangle &= \sum_{\alpha,\beta} c_{\alpha\beta} e^{i(\Theta_{\alpha\beta} + \Theta_{\alpha'\beta'})} (e^{i\bar{\nu}})^{\alpha\beta + \delta_{\alpha'\beta'} - \alpha'\beta'} |\alpha'\beta\rangle. \end{aligned}$$

All the summations run over  $\alpha, \beta = 0, 1$ , we used the notation  $\alpha' \equiv 1 - \alpha$ ,  $\beta' \equiv 1 - \beta$  and applied the approximation

$$(1 + \zeta)^m \simeq 1 + m\zeta, \quad \zeta \ll 1. \quad (\text{C4})$$

In what follows we neglect terms of the second and higher orders in  $\zeta$  denoted as  $\mathcal{O}(\zeta^2)$ .

Substituting Eq. (C3) into Eq. (50) the fidelity of the phase gate with the imperfect  $\pi$  pulses is

$$\begin{aligned} \tilde{\mathcal{F}} &\simeq \left\langle \min_{\{c_{\alpha\beta}\}} \left\{ (1 - 4\zeta) \left| \sum_{\alpha,\beta} |c_{\alpha\beta}|^2 e^{i(\delta\Theta_{\alpha\beta} + \delta\Theta_{\alpha'\beta'})} \right|^2 \right. \right. \\ &\quad + \zeta \left| (K - N) e^{i(\delta\Theta_{00} + \delta\Theta_{11})} + (K^* - N^*) e^{i(\delta\Theta_{01} + \delta\Theta_{10})} \right|^2 \\ &\quad + \zeta \left| (L - M) e^{i(\delta\Theta_{00} + \delta\Theta_{11})} + (L^* - M^*) e^{i(\delta\Theta_{01} + \delta\Theta_{10})} \right|^2 \\ &\quad + \zeta \left| (K - iN^*) e^{i(\delta\Theta_{00} + \delta\Theta_{10})} + (K^* + iN) e^{i(\delta\Theta_{01} + \delta\Theta_{11})} \right|^2 \\ &\quad \left. \left. + \zeta \left| (L - iM^*) e^{i(\delta\Theta_{00} + \delta\Theta_{01})} + (L^* + iM) e^{i(\delta\Theta_{10} + \delta\Theta_{11})} \right|^2 \right\} \right\rangle \end{aligned} \quad (\text{C5})$$

where  $\{K, L, M, N\} \equiv \{c_{00} c_{01}^*, c_{00} c_{10}^*, c_{11} c_{01}^*, c_{11} c_{10}^*\}$  and  $\alpha, \beta = 0, 1$ . The first term in Eq. (C5) is equal (up to the factor  $1 - 4\zeta$ ) to the fidelity of the gate with the perfect  $\pi$  pulses expressed by Eq. (28). The other four terms in Eq. (C5) have always a non-negative contribution. We can find an initial state (i.e. a combination of coefficients  $c_{\alpha\beta}$ ) which makes the contribution of these four terms equal to zero, thus minimising the expression in Eq. (C5). Then the fidelity of the phase gate with imperfect  $\pi$  pulses is as given in Eq. (51).

### APPENDIX D: FORCED CLASSICAL HARMONIC OSCILLATOR

We treat the ion system semiclassically, in that we assume internal ionic states  $|0\rangle$  and  $|1\rangle$  but we treat the motion of the ions as a motion of classical particles. Then, the motion of a single classical particle confined in a harmonic potential with an external force is described by the Lagrangian

$$L(t) = \frac{1}{2} m \dot{x}^2 - \left[ \frac{1}{2} m \omega^2 x^2 - xF(t) \right], \quad (\text{D1})$$

where  $x(t)$  denotes the trajectory of the particle,  $F(t)$  is a time-dependent external force and  $\dot{x} = dx/dt$ . We can rewrite the Lagrangian (D1) in the form

$$L(t) = \frac{1}{2} m \dot{x}^2 - \frac{1}{2} m \omega^2 (x - \bar{x})^2 - \frac{1}{2} m \omega^2 \bar{x}^2, \quad (\text{D2})$$

where

$$\bar{x}(t) = F(t)/m\omega^2. \quad (\text{D3})$$

It follows from Eq. (D1) and (D2) that the action of the force on the particle corresponds to the time-dependent displacement (D3) of the harmonic potential in which the particle is confined. The dynamics of the particle are given by the Lagrange equation

$$\frac{d}{dt} \frac{\partial L}{\partial \dot{x}} - \frac{\partial L}{\partial x} = 0. \quad (\text{D4})$$

Substituting the Lagrangian (D2) into Eq. (D4) we get the equation of motion

$$\ddot{x}(t) + \omega^2 x(t) = F(t)/m, \quad (\text{D5})$$

which can be solved analytically. The solution splits into three terms

$$x(t) = \bar{x}(t) - \delta(t) + \Delta(t), \quad (\text{D6})$$

where  $\bar{x}(t)$  is the time-dependent displacement of the potential defined in Eq. (D3),  $\delta(t)$  is so called *slushing motion*

$$\begin{aligned} \delta(t) = & \sin(\omega t) \left[ \int_{t_0}^t \dot{\bar{x}}(t') \sin(\omega t') dt' \right] \\ & + \cos(\omega t) \left[ \int_{t_0}^t \dot{\bar{x}}(t') \cos(\omega t') dt' \right], \end{aligned} \quad (\text{D7})$$

and finally  $\Delta(t)$  denotes standard oscillations of the particle confined in the harmonic potential

$$\Delta(t) = (x_0 - \bar{x}_0) \cos(\omega t) + (\dot{x}_0/\omega) \sin(\omega t), \quad (\text{D8})$$

where the initial conditions are  $x_0 = x(t_0)$ ,  $\bar{x}_0 = \bar{x}(t_0)$  and  $\dot{x}_0 = \frac{dx}{dt}(t_0)$ . We can rewrite Eq. (D8) in the form

$$\Delta(t) = \sqrt{2\mathcal{E}/m\omega^2} \cos(\omega t + \psi), \quad (\text{D9})$$

where  $\mathcal{E}$  is the oscillation energy of the particle in the harmonic potential and  $\psi$  is the initial phase which depends on initial conditions.

We can assume that the ion experiences a harmonic potential only in the limit  $\epsilon \ll 1$ . Otherwise, Eq. (D6) does not describe its motion or describes it only approximately.

## APPENDIX E: TWO-PARTICLE INTERACTION PHASES

It is sufficient to consider in Eq. (80) with respect to assumptions (i)–(iii) only the terms up to  $n = 4$  and we choose  $|t_0|, |t| \rightarrow \infty$  (except for global phases) for the same reason as it is stated in Eq. (76). Then we can have (swapping integration and summation)

$$\phi_{\alpha\beta} \approx \phi_{\alpha\beta}^{(0)} + \sum_{n=1}^4 \phi_{\alpha\beta}^{(n)}, \quad (\text{E1})$$

where

$$\phi_{\alpha\beta}^{(n)} = -\frac{\ell}{\hbar d} \int_{-\infty}^{+\infty} \left[ \frac{x_\alpha(t) - x'_\beta(t)}{d} \right]^n dt, \quad (\text{E2})$$

and  $\phi_{\alpha\beta}^{(0)} = -(\ell/\hbar d)(t - t_0)$  is a global phase. Using Eq. (68) the motion of ion 1 in the internal state  $|\alpha\rangle$  and ion 2 in the state  $|\beta\rangle$  can be expressed (when  $\epsilon \ll 1$ ) as follows

$$x_\alpha(t) = \bar{x}_\alpha(t) + \Delta(t), \quad (\text{E3a})$$

$$x'_\beta(t) = \bar{x}'_\beta(t) + \Delta'(t), \quad (\text{E3b})$$

where the time-dependent displacements  $x_\alpha(t)$  and  $x'_\beta(t)$  are defined by Eq. (62) while the oscillations in the microtraps (Eq. (D9)) are

$$\Delta(t) = \sqrt{\frac{2\mathcal{E}_1}{m\omega^2}} \cos(\omega t + \psi_1), \quad (\text{E4a})$$

$$\Delta'(t) = \sqrt{\frac{2\mathcal{E}_2}{m\omega^2}} \cos(\omega t + \psi_2). \quad (\text{E4b})$$

The parameters  $\mathcal{E}_1$  and  $\mathcal{E}_2$  are oscillations energies of the ions which are in principle different because the ions are trapped in two separate and independent potentials. Using Eq. (E3) and (E4) we can express Eq. (E2) in the form

$$\phi_{\alpha\beta}^{(n)} = -\frac{\ell}{\hbar d} \int_{-\infty}^{+\infty} \left[ \frac{(\alpha - \beta)a\mathcal{F} + (\Delta - \Delta')}{d} \right]^n dt. \quad (\text{E5})$$

When we now neglect in the adiabatic approximation (67) all terms where the factor  $e^{-(\omega\tau)^2}$  appears, then we can express the linear term ( $n = 1$ ) from Eq. (E5) as follows

$$\phi_{\alpha\beta}^{(1)} = -\frac{\sqrt{\pi}}{4} (\alpha - \beta)\epsilon\omega\tau\xi \frac{d}{a} + Q_1, \quad (\text{E6})$$

where  $\alpha, \beta = 0, 1$ ,  $\epsilon$  is defined by Eq. (70),  $\xi$  and  $\tau$  are introduced in Eq. (66),  $\omega$  is the oscillation frequency with respect to Eq. (71),  $d$  is the ion separation with respect to Eq. (69),  $a$  is defined in Eq. (58) and for global phases we used the notation

$$Q_n = -\frac{\ell}{\hbar d} \int_{t_0}^t \left( \frac{\Delta - \Delta'}{d} \right)^n dt'. \quad (\text{E7})$$

The quadratic term ( $n = 2$ ) reads

$$\phi_{\alpha\beta}^{(2)} = -\sqrt{\frac{\pi}{32}} (\alpha - \beta)^2 \epsilon\omega\tau\xi^2 + Q_2, \quad (\text{E8})$$

the cubic term ( $n = 3$ ) reads

$$\begin{aligned} \phi_{\alpha\beta}^{(3)} &= -\sqrt{\frac{\pi}{48}} (\alpha - \beta)^3 \epsilon \omega \tau \xi^3 \frac{a}{d} \\ &\quad - \frac{3}{4} \sqrt{\pi} (\alpha - \beta) \epsilon \omega \tau \xi \frac{a}{d} \times \\ &\quad \times \left[ \frac{\mathcal{E}_1}{\hbar\omega} + \frac{\mathcal{E}_2}{\hbar\omega} - 2 \frac{\sqrt{\mathcal{E}_1 \mathcal{E}_2}}{\hbar\omega} \cos(\psi_1 - \psi_2) \right] + Q_3 \end{aligned} \quad (\text{E9})$$

and finally the biquadratic term ( $n = 4$ ) reads

$$\begin{aligned} \phi_{\alpha\beta}^{(4)} &= -\sqrt{\frac{\pi}{8}} (\alpha - \beta)^4 \epsilon \omega \tau \xi^4 \left(\frac{a}{d}\right)^2 \\ &\quad - \sqrt{\frac{9\pi}{8}} (\alpha - \beta)^2 \epsilon \omega \tau \xi^2 \left(\frac{a}{d}\right)^2 \times \\ &\quad \times \left[ \frac{\mathcal{E}_1}{\hbar\omega} + \frac{\mathcal{E}_2}{\hbar\omega} - 2 \frac{\sqrt{\mathcal{E}_1 \mathcal{E}_2}}{\hbar\omega} \cos(\psi_1 - \psi_2) \right] + Q_4, \end{aligned} \quad (\text{E10})$$

where  $\mathcal{E}_1, \mathcal{E}_2$  and  $\psi_1, \psi_2$  are associated with oscillations of the ions in the microtraps and they are defined in Eq. (E4).

When we substitute Eq. (82) into Eq. (E6)–(E10) we can write the interaction phases  $\phi_{\alpha\beta}$  in Eq. (75) with the precision up to  $n = 4$  in a compact form

$$\begin{aligned} \phi_{\alpha\beta} &= -(\alpha - \beta) \theta \frac{d}{a} \frac{1}{\xi \sqrt{2}} - (\alpha - \beta)^2 \theta \frac{1}{2} \\ &\quad - (\alpha - \beta)^3 \theta \frac{a}{d} \left\{ \frac{\xi}{\sqrt{6}} + \frac{3}{\xi \sqrt{2}} \times \right. \\ &\quad \times \left. \left[ \frac{\mathcal{E}_1}{\hbar\omega} + \frac{\mathcal{E}_2}{\hbar\omega} - 2 \frac{\sqrt{\mathcal{E}_1 \mathcal{E}_2}}{\hbar\omega} \cos(\psi_1 - \psi_2) \right] \right\} \\ &\quad - (\alpha - \beta)^4 \theta \left(\frac{a}{d}\right)^2 \left\{ \frac{\xi^2}{\sqrt{8}} + \right. \\ &\quad \left. + 3 \left[ \frac{\mathcal{E}_1}{\hbar\omega} + \frac{\mathcal{E}_2}{\hbar\omega} - 2 \frac{\sqrt{\mathcal{E}_1 \mathcal{E}_2}}{\hbar\omega} \cos(\psi_1 - \psi_2) \right] \right\}. \end{aligned} \quad (\text{E11})$$

The mean (estimated) value of the phases  $\phi_{\alpha\beta}$  with respect to Eq. (84) is

$$\begin{aligned} \bar{\phi}_{\alpha\beta} &= -(\alpha - \beta) \theta \frac{d}{a} \frac{1}{\xi \sqrt{2}} - (\alpha - \beta)^2 \theta \frac{1}{2} \\ &\quad - (\alpha - \beta)^3 \theta \frac{a}{d} \left( \frac{\xi}{\sqrt{6}} + \frac{1}{\xi \sqrt{2}} \frac{6k_B T}{\hbar\omega} \right) \\ &\quad - (\alpha - \beta)^4 \theta \left(\frac{a}{d}\right)^2 \left( \frac{\xi^2}{\sqrt{8}} + \frac{6k_B T}{\hbar\omega} \right). \end{aligned} \quad (\text{E12})$$

Now we can easily calculate the difference between the actual and the estimated value of the phase  $\phi_{\alpha\beta}$  which

appears in the expression for the fidelity of the gate in Eq. (20) and (28). We will find out (in the approximation when we ignore fluctuations of the pushing force) that the fidelity of the gate is determined by the terms of the order  $n = 3$  and  $n = 4$  which represent thermal corrections to the motion of the ions.

## APPENDIX F: NON-UNIFORM PUSHING FORCE: FIDELITY

It follows from Eq. (36) and (37) that the fidelity of the phase gate with  $\pi$  pulses is given for  $\delta\vartheta \ll 1$  as

$$\mathcal{F}' = \left\langle \frac{1}{2} [1 + \cos(\delta\vartheta)] \right\rangle \approx 1 - \frac{1}{4} \langle (\delta\vartheta)^2 \rangle, \quad (\text{F1})$$

where  $\langle \cdot \rangle$  denotes averaging as stated in Eq. (120). Before we calculate the fidelity it is convenient to relabel the quantity  $\theta$ , originally defined in Eq. (82), giving

$$\theta = \left( \sqrt{\frac{\pi}{8}} \epsilon \omega \tau \xi_0^2 \right) \frac{\xi^2}{\xi_0^2} = \theta_0 \frac{\xi^2}{\xi_0^2}, \quad (\text{F2})$$

where  $\xi_0$  refers to the amplitude of the force at  $x = 0$  ( $z = 0$ ) and  $\xi = \xi_{\text{trav}}(x)$  or  $\xi = \xi_{\text{stan}}(z)$ , respectively. Carrying out the averaging in Eq. (F1) the fidelity of the phase gate with  $\pi$  pulses for the non-unitary pushing force up to  $(a/d)^4$  is found to be

$$\begin{aligned} \mathcal{F}' &= 1 - \frac{\theta_0^2}{4\xi_0^4} \left\{ [\bar{\xi}^4 - (\bar{\xi}^2)^2] \right. \\ &\quad + \left(\frac{a}{d}\right)^2 \left[ 2 \left( \frac{12k_B T}{\hbar\omega} \right) [\bar{\xi}^4 - (\bar{\xi}^2)^2] + \frac{2}{\sqrt{2}} (\bar{\xi}^6 - \bar{\xi}^2 \bar{\xi}^4) \right] \\ &\quad + \left(\frac{a}{d}\right)^4 \left[ \left( \frac{12k_B T}{\hbar\omega} \right)^2 [2\bar{\xi}^4 - (\bar{\xi}^2)^2] + \frac{2}{\sqrt{2}} \left( \frac{12k_B T}{\hbar\omega} \right) \times \right. \\ &\quad \left. \times (\bar{\xi}^6 - \bar{\xi}^2 \bar{\xi}^4) + \frac{1}{2} [\bar{\xi}^8 - (\bar{\xi}^4)^2] \right] \left. \right\}, \end{aligned} \quad (\text{F3})$$

where

$$\bar{\xi}^n \equiv \int_{-\infty}^{+\infty} dx \xi^n(x) P(x). \quad (\text{F4})$$

To calculate the quantity  $\bar{\xi}^n$  which appears in the expression for the fidelity, we use Eq. (118) for the case of the travelling wave. Then, in the limit  $r \ll 1$ , where we introduce the coefficient  $r \equiv 2\sigma/w \approx 2a\sqrt{\langle n \rangle}/w$ , we find

$$\bar{\xi}^n \approx \xi_0^n \left[ 1 + r^2 A^{(n)} + r^4 B^{(n)} \right]. \quad (\text{F5})$$

We will consider also the term of the order of  $r^4$  because it scales with  $(a/w)^4$  and it is comparable with or larger than  $(a/d)^4$ . Finally, we need to evaluate the coefficients

$A^{(n)}$  and  $B^{(n)}$  for  $n = 2, 4, 6, 8$ . They are

$$A^{(2)} = \frac{1}{R^2} + 2R^2 - 5, \quad (\text{F6a})$$

$$B^{(2)} = -\frac{3}{R^2} + \frac{39}{2} - 14R^2 + 2R^4,$$

$$A^{(4)} = \frac{6}{R^2} + 8R^2 - 18, \quad (\text{F6b})$$

$$B^{(4)} = \frac{3}{R^4} - \frac{84}{R^2} + 246 - 176R^2 + 32R^4,$$

$$A^{(6)} = \frac{15}{R^2} + 18R^2 - 39, \quad (\text{F6c})$$

$$B^{(6)} = \frac{45}{R^4} - \frac{495}{R^2} + \frac{2295}{2} - 810R^2 + 162R^4,$$

$$A^{(8)} = \frac{28}{R^2} + 32R^2 - 68, \quad (\text{F6d})$$

$$B^{(8)} = \frac{210}{R^4} - \frac{1680}{R^2} + 3480 - 2432R^2 + 512R^4,$$

where we denoted  $R \equiv 2x_0/w$ . It is of the order of one ( $R \sim 1$ ) because  $x_0$  refers to the position of the ion in the laser beam and hence we can assume  $x_0 \sim w$ .

By similar means, we can calculate  $\xi^n$  for the case of the standing wave. Substituting Eq. (119) into Eq. (F4) we get

$$\bar{\xi}^2 = \frac{\xi_0^2}{2 \sin^2(2kz_0)} \left[ 1 - e^{-8(k\sigma)^2} \cos(4kz_0) \right], \quad (\text{F7a})$$

$$\begin{aligned} \bar{\xi}^4 = \frac{\xi_0^4}{8 \sin^4(2kz_0)} & \left[ 3 - 4e^{-8(k\sigma)^2} \cos(4kz_0) \right. \\ & \left. + e^{-32(k\sigma)^2} \cos(8kz_0) \right], \end{aligned} \quad (\text{F7b})$$

$$\begin{aligned} \bar{\xi}^6 = \frac{\xi_0^6}{32 \sin^6(2kz_0)} & \left[ 10 - 15e^{-8(k\sigma)^2} \cos(4kz_0) \right. \\ & \left. + 6e^{-32(k\sigma)^2} \cos(8kz_0) - e^{-72(k\sigma)^2} \cos(12kz_0) \right], \end{aligned} \quad (\text{F7c})$$

$$\begin{aligned} \bar{\xi}^8 = \frac{\xi_0^8}{128 \sin^8(2kx_0)} & \left[ 35 - 56e^{-8(k\sigma)^2} \cos(4kz_0) \right. \\ & \left. + 28e^{-32(k\sigma)^2} \cos(8kz_0) - 8e^{-72(k\sigma)^2} \cos(12kz_0) \right. \\ & \left. + e^{-128(k\sigma)^2} \cos(16kz_0) \right]. \end{aligned} \quad (\text{F7d})$$

It is useful to write the exponents in Eq. (F7) in the form

$$(k\sigma)^2 \approx 2\eta^2 \langle n \rangle, \quad (\text{F8})$$

where  $\eta = ka/\sqrt{2}$  is so called *Lamb-Dicke parameter*,  $k = 2\pi/\lambda$  is the wavenumber of the laser light and all other constants are defined in Eq. (123). Then, we distinguish two extreme cases: (i) Lamb-Dicke regime ( $\eta^2 \langle n \rangle \ll 1$ ) and (ii) outside the Lamb-Dicke regime ( $\eta^2 \langle n \rangle \gtrsim 1$ ). The former case corresponds to the situation where the spatial extent of the vibrational motion of the ion is much smaller than the wavelength of the laser light ( $a\sqrt{\langle n \rangle} \ll \lambda$ ). It means that the ion is cold enough to be well localized in the standing-wave and not to travel across its nodes and antinodes. In other words, in the Lamb-Dicke regime the ion does not experience the non-uniform profile of the standing wave. Then, we have  $e^{-(k\sigma)^2} \rightarrow 1$ , giving  $\xi^n \rightarrow \xi_0^n$  and the fidelity (F3) reduces to Eq. (88) which describes the case of the uniform pushing force.

Outside the Lamb-Dicke regime we have the situation where  $e^{-(k\sigma)^2} \rightarrow 0$  and it leaves us only with the first terms in Eqs. (F7). In the expression for the fidelity (F3) the first term dominates, giving

$$\mathcal{F}' \approx 1 - \frac{\theta_0^2}{4\xi_0^2} [\bar{\xi}^4 - (\bar{\xi}^2)^2] = 1 - \frac{\theta_0^2}{32 \sin^4(2kz_0)}. \quad (\text{F9})$$

The condition for the phase gate gives  $2\theta_0 \approx \pi$  and we choose  $kz_0 = \pi/4$ , then  $\mathcal{F}' \approx 0.92$ .

---

[1] I. Cirac and P. Zoller, Phys. Rev. Lett. **74**, 4091 (1995)  
[2] Fortschr. Phys. **48**, 769 – 1138 (2000)  
[3] A. Steane, Appl. Phys. B**64**, 623 (1997)  
[4] D. Wineland *et al.*, Jour. Nat. Inst. Stand. Technol. **103**, 259 (1998)  
[5] Ch. Nägerl *et al.*, Fortschr. Phys. **48**, 623 (2000)  
[6] M. Šašura and V. Bužek, Jour. Mod. Opt. **49**, 1593

(2002)  
[7] I. Cirac and P. Zoller, Nature **404**, 579 (2000)  
[8] T. Calarco, I. Cirac and P. Zoller, Phys. Rev. A **63**, 062304 (2001)  
[9] A. Barenco *et al.*, Phys. Rev. A **52**, 3457 (1995)  
[10] H. J. Metcalf and P. van der Straten, *Laser cooling and trapping*, Springer-Verlag, New York (1999)



[11] M. Šašura, A. Steane *et al.*, in preparation

[12] A. Steane *et al.* Phys. Rev. A **62**, 042305 (2000)

[13] A. Sørensen and K. Mølmer, Phys. Rev. Lett. **82**, 1971 (1999)

[14] A. Sørensen and K. Mølmer, Phys. Rev. A **62**, 022311

(2000)

[15] D. Jonathan, M. Plenio and P. L. Knight, Phys. Rev. A **62**, 042307 (2000)